# How Crystals are Grown

R. K. Route, S. Rowan, E. K. Gustafson
and M. M. Fejer

Galileo Group, Stanford University

LSC Meeting
4-6 March 1999
Florida

## SINGLE CRYSTALS

## [illegible]

## [illegible] FI[illegible]

## GLASSES

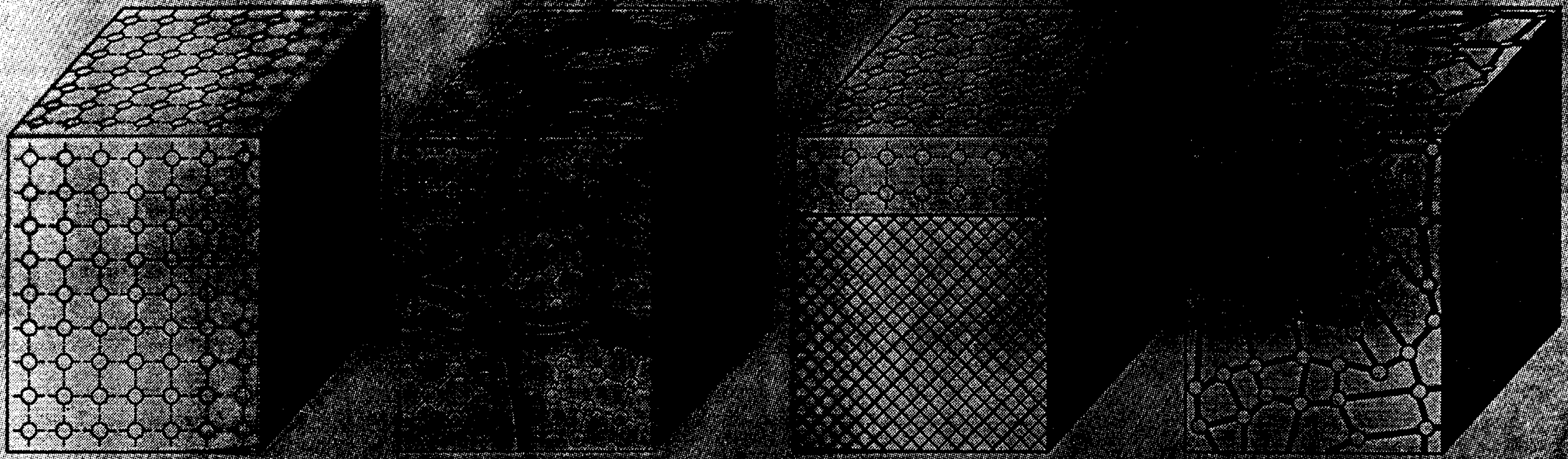

Those with a [illegible] configuration of atoms

[illegible]

[illegible]

[illegible] egular [illegible] atoms

# Crystal Growth Methods

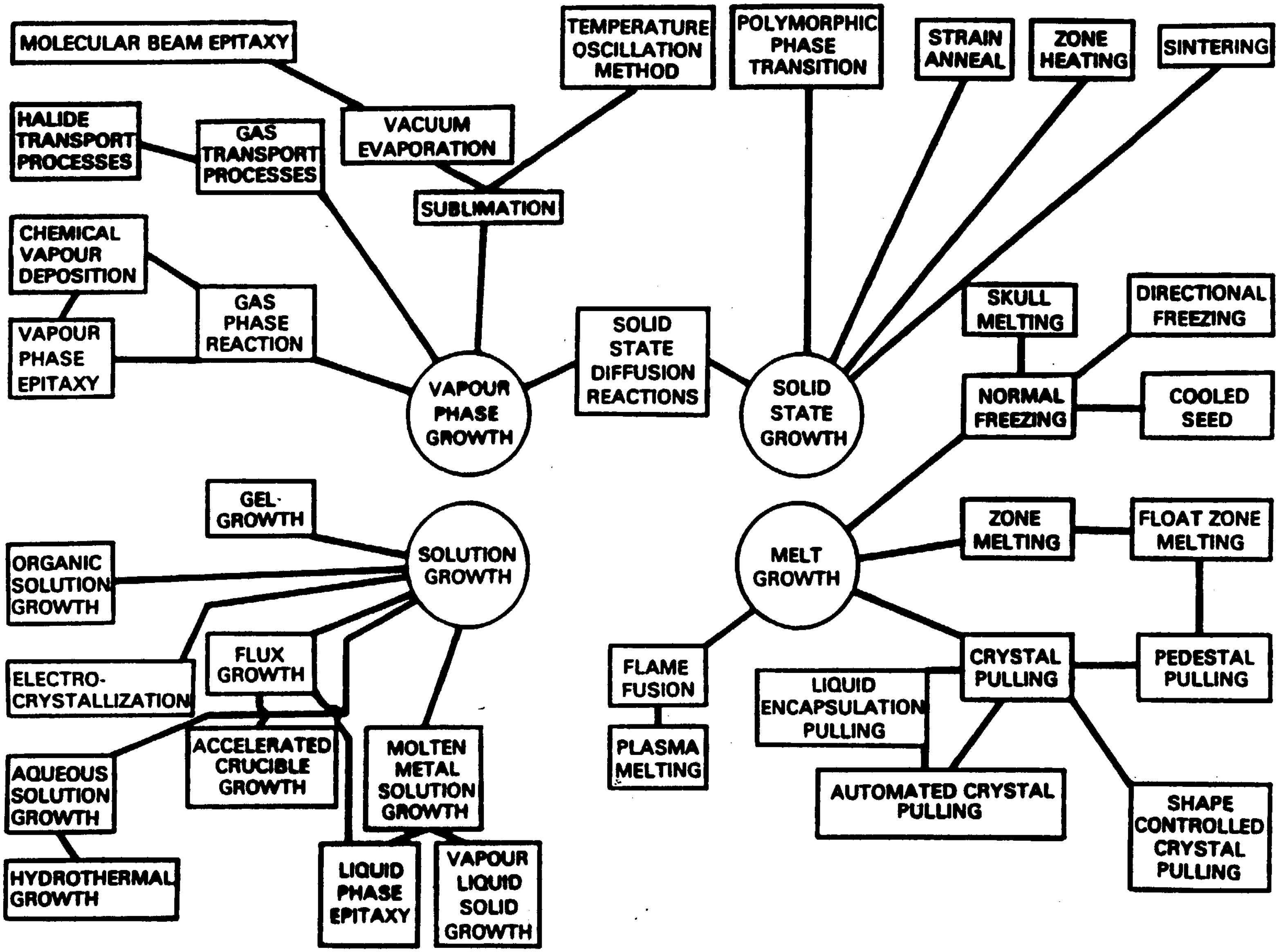

MOLECULAR BEAM EPITAXY

TEMPERATURE OSCILLATION METHOD

POLYMORPHIC PHASE TRANSITION

STRAIN ANNEAL

ZONE HEATING

SINTERING

HALIDE TRANSPORT PROCESSES

GAS TRANSPORT PROCESSES

VACUUM EVAPORATION

SUBLIMATION

CHEMICAL VAPOUR DEPOSITION

GAS PHASE REACTION

VAPOUR PHASE EPITAXY

SKULL MELTING

DIRECTIONAL FREEZING

SOLID STATE DIFFUSION REACTIONS

VAPOUR PHASE GROWTH

SOLID STATE GROWTH

NORMAL FREEZING

COOLED SEED

GEL GROWTH

ORGANIC SOLUTION GROWTH

SOLUTION GROWTH

MELT GROWTH

ZONE MELTING

FLOAT ZONE MELTING

ELECTRO-CRYSTALLIZATION

FLUX GROWTH

FLAME FUSION

LIQUID ENCAPSULATION PULLING

CRYSTAL PULLING

PEDESTAL PULLING

AQUEOUS SOLUTION GROWTH

ACCELERATED CRUCIBLE GROWTH

MOLTEN METAL SOLUTION GROWTH

PLASMA MELTING

AUTOMATED CRYSTAL PULLING

SHAPE CONTROLLED CRYSTAL PULLING

HYDROTHERMAL GROWTH

LIQUID PHASE EPITAXY

VAPOUR LIQUID SOLID GROWTH

# Materials of Interest to LIGO

- Growable in sizes required
- Possess appropriate optical and mechanical properties
  - Fused Silica ($SiO_2$) - Amorphous, optically isotropic
  - Sapphire ($Al_2O_3$) - Trigonal $\bar{3}m$, optically uniaxial
  - Silicon - Cubic $\bar{4}3m$, optically isotropic in mid-IR
  - YAG ($Y_3Al_5O_{12}$) - Cubic m3m, optically isotropic but most boules exhibit strain birefringence under iconoscope
  - Spinel ? ($MgAl_2O_4$) - Cubic m3m , optically isotropic but not grown commercially, evaporates incongruently (preferentially loses MgO)

# Natural Habits of LIGO Materials

**Sapphire - $D_{3d}$-$\bar{3}m$**

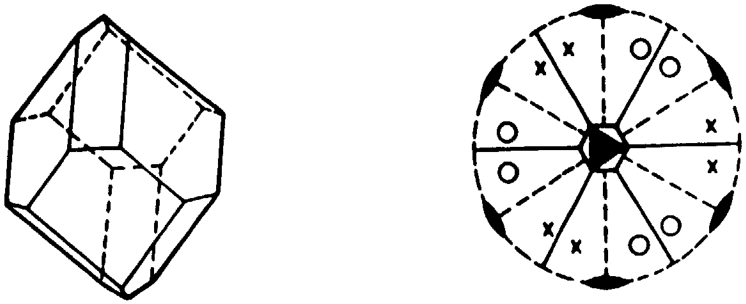

**YAG and Spinel - $O_h$-m3m**

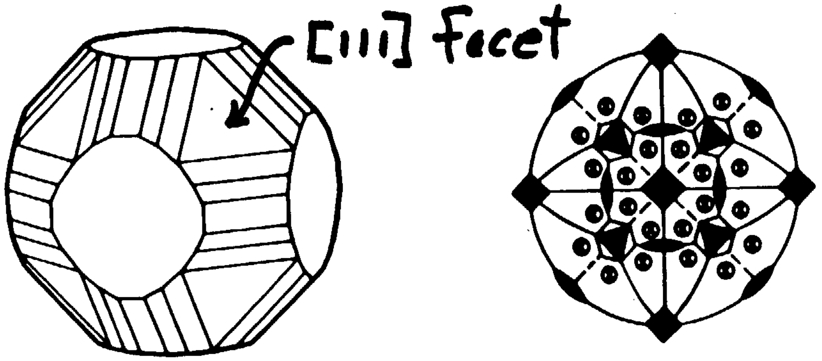

**Silicon - $T_d$-$\bar{4}3m$**

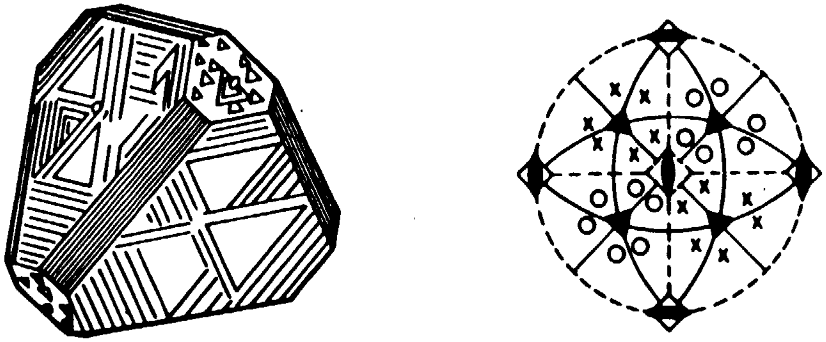

# Properties of Crystalline Materials

| Material | Melting Point (°C) | Melt Growth Method | Crucible Materials | Knoop Hardness (Kg/mm$^2$) |
|---|---|---|---|---|
| fused silica | 1710 | casting | | 635 |
| sapphire | 2050 | Cz, HEM, V, EFG | Ir, Mo, W | >2000 |
| YAG | 1950 | Cz, HEM | Ir, Mo | 1350 |
| spinel | 2135 | Cz, HEM, V | Mo | >1500 |
| silicon | 1410 | Cz, HEM, Web | $SiO_2$, PBN | 1150 |
| platinum | 1770 | | | |
| iridium | 2454 | | | |
| moly | 2610 | | | |
| tungsten | 3410 | | | |

Except for fused silica, all melt congruently,
none suffer reconstructive phase transitions,
none are highly volatile.

- Well suited to melt growth techniques -

# Phase Diagrams

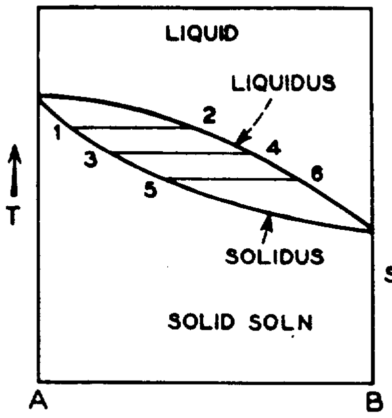

(a)

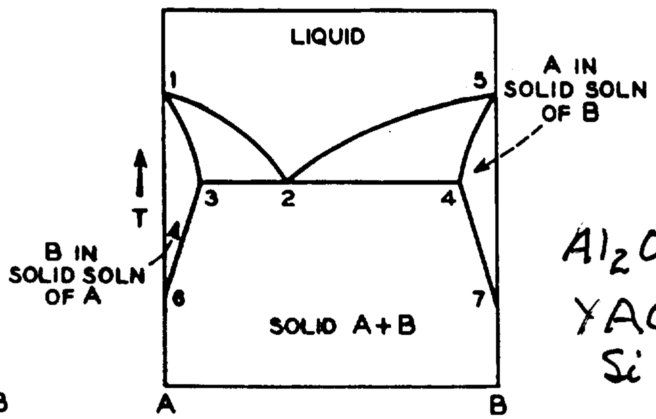

(b)

$Al_2O_3$
YAG
Si

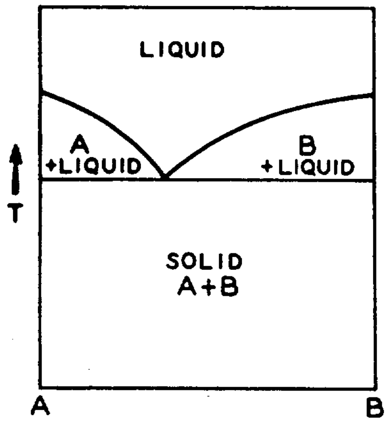

(c)

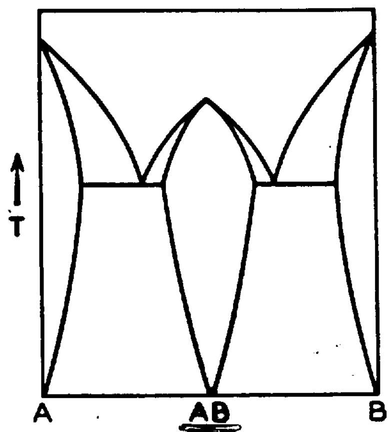

(d)

Spinel

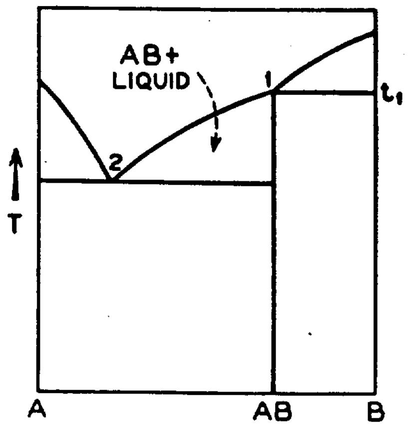

(e)

# Distribution Coefficient

$$k_0\,(X_1) = \frac{ab}{ac}$$

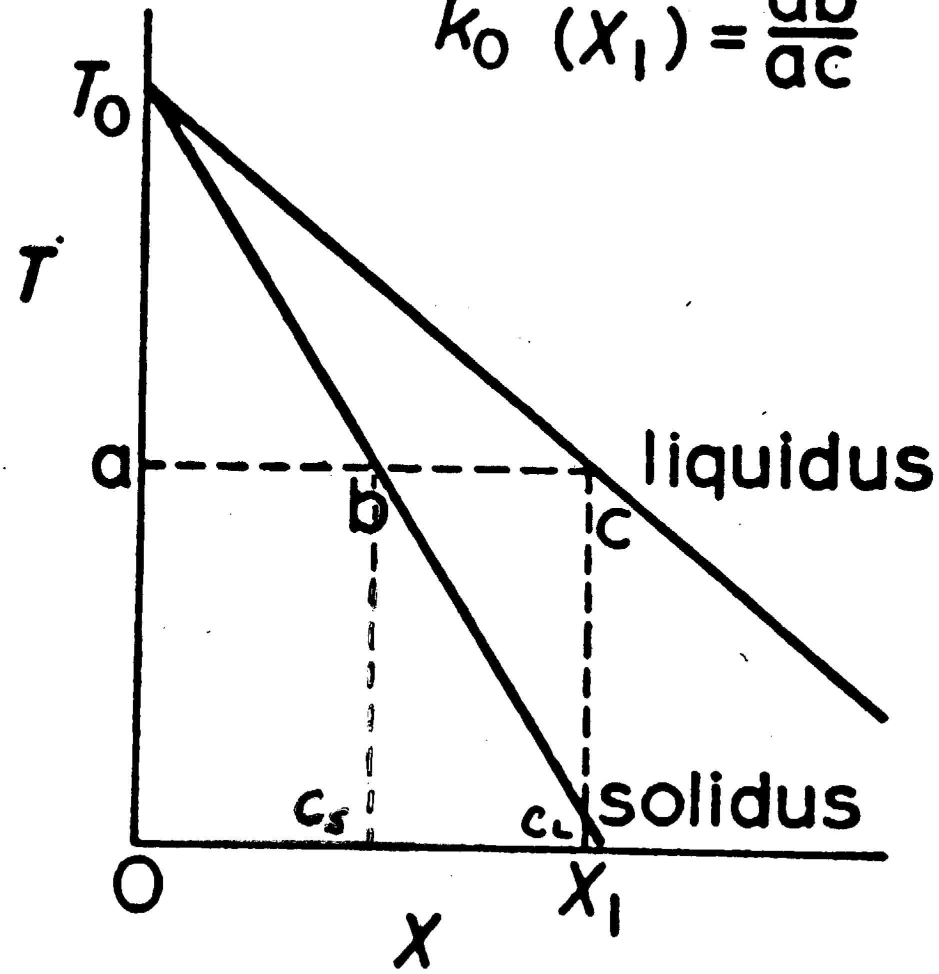

# Growth Stability

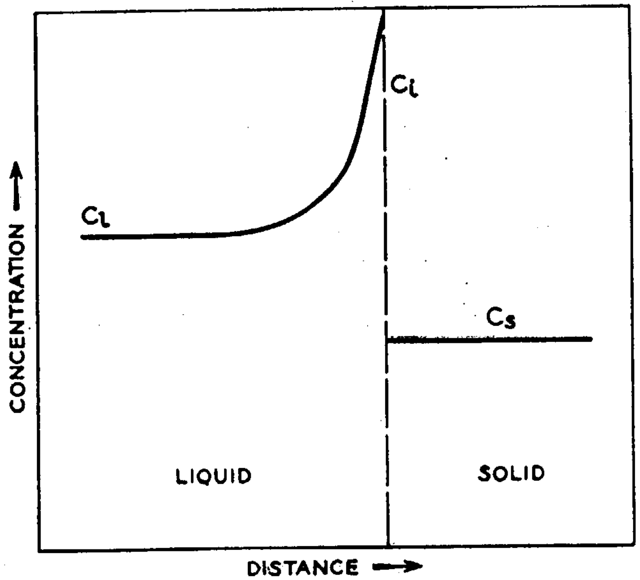

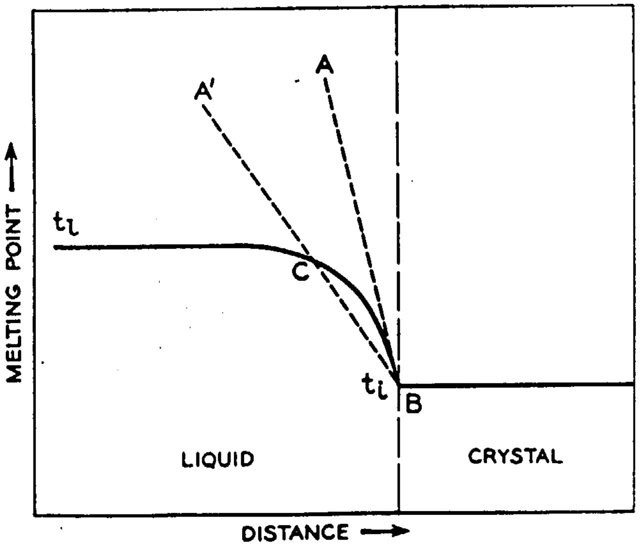

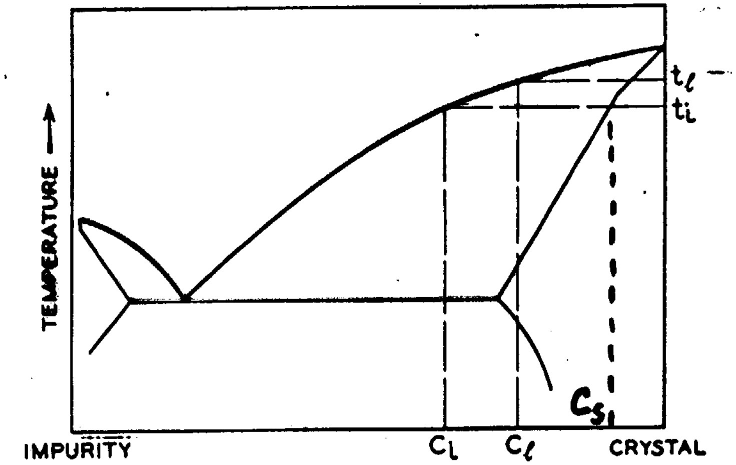

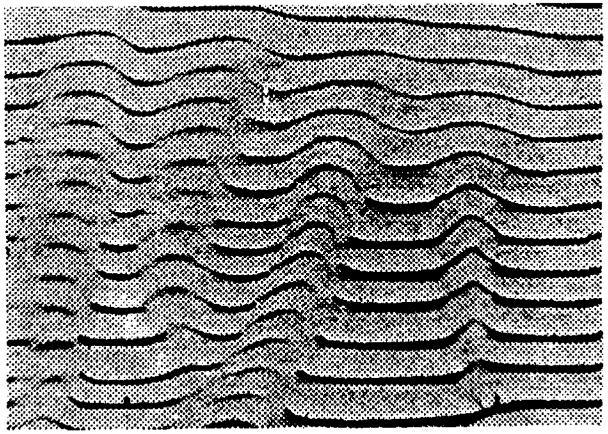

# Crystal Pulling

## Czochralski, Kyropoulus

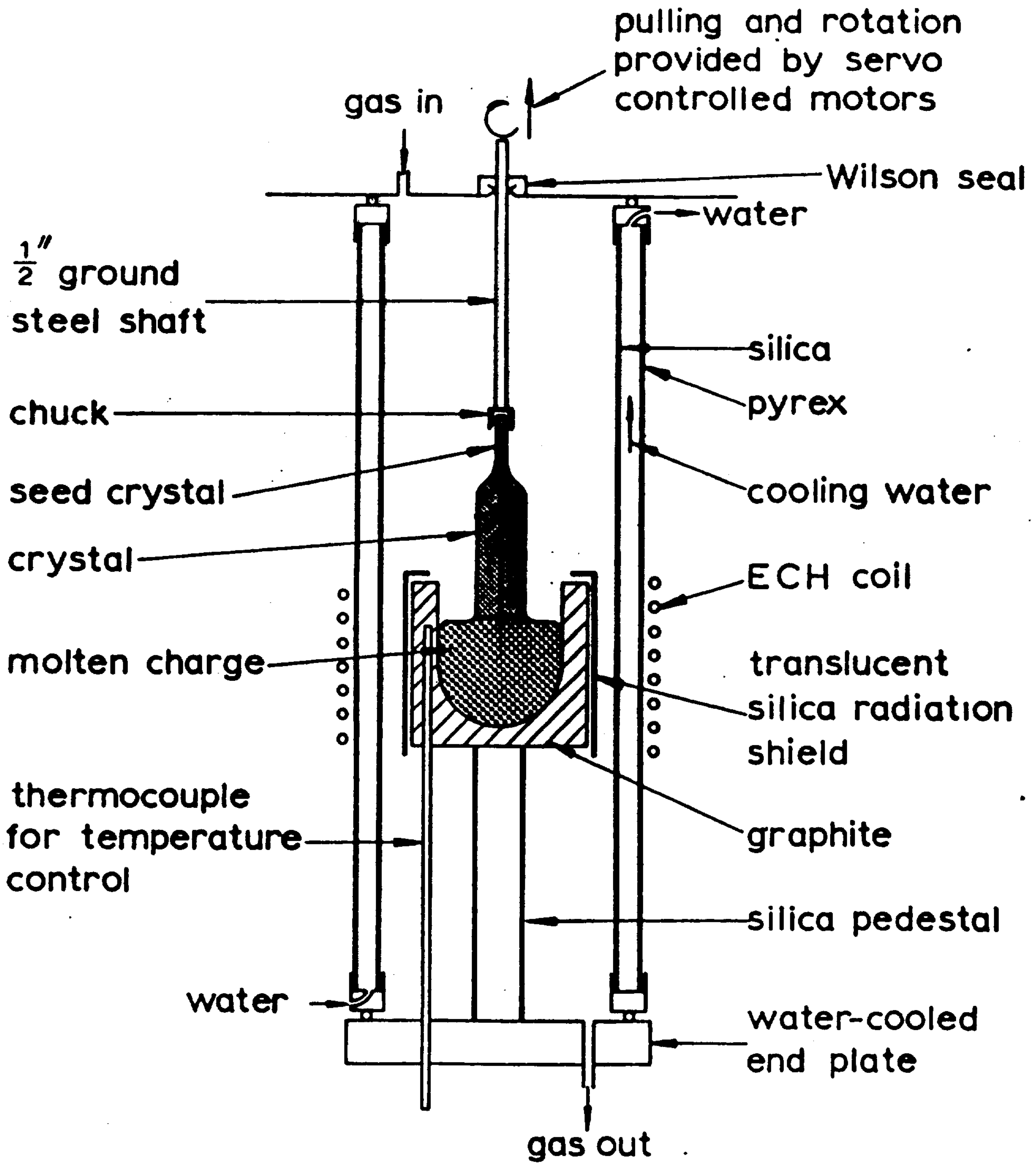

# Unidirectional Solidification

**Bridgman, Gradient Freeze, HEM**

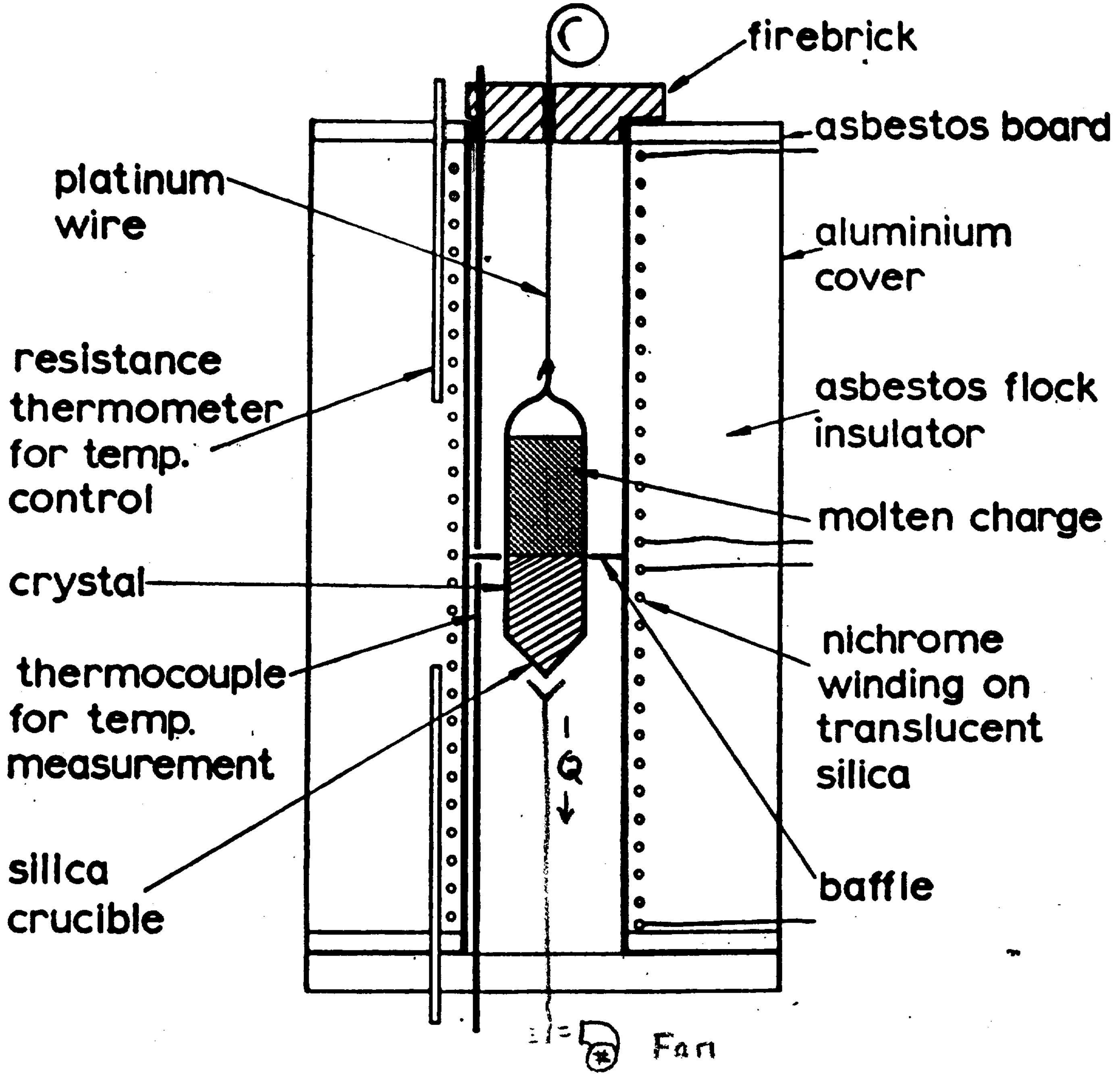

# Zone Melting

## Float Zone, Zone Refining, Travelling Zone

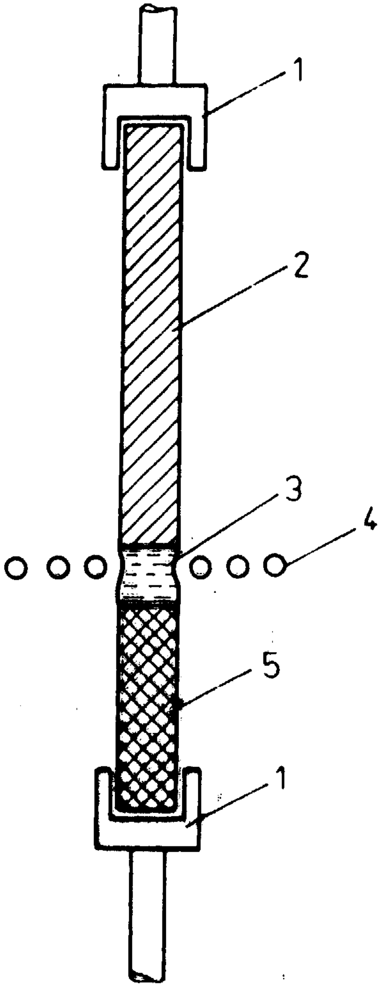

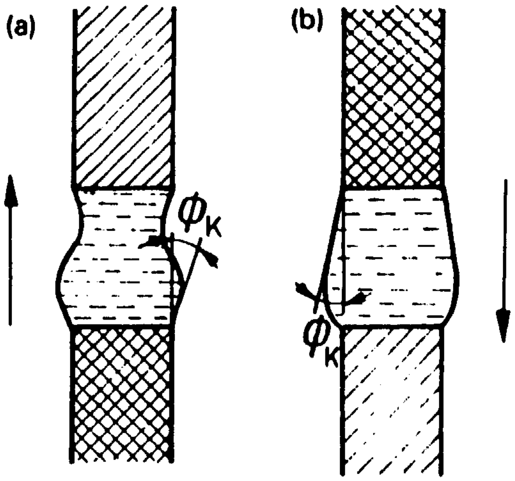

# Czochralski Growth Method

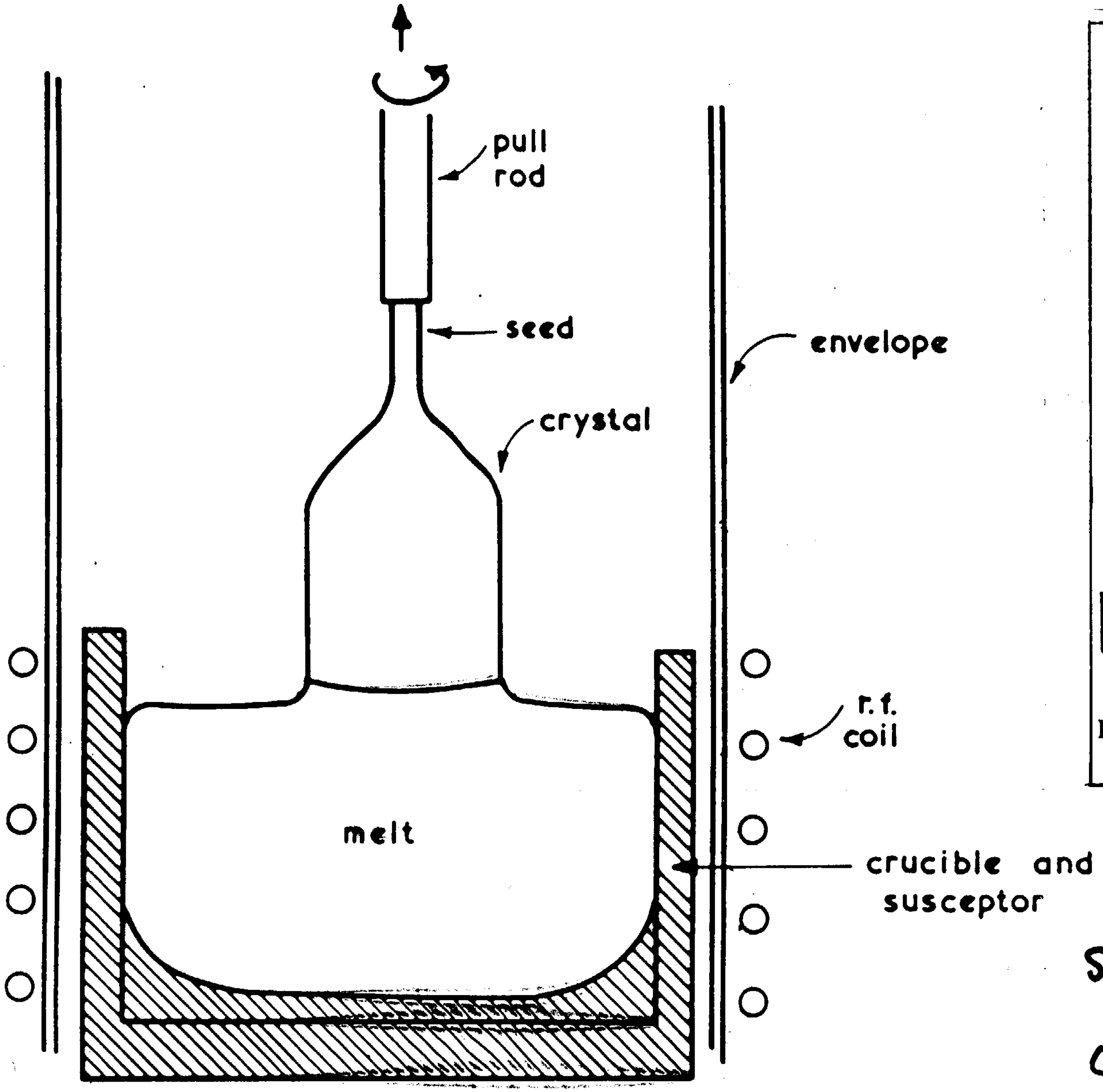

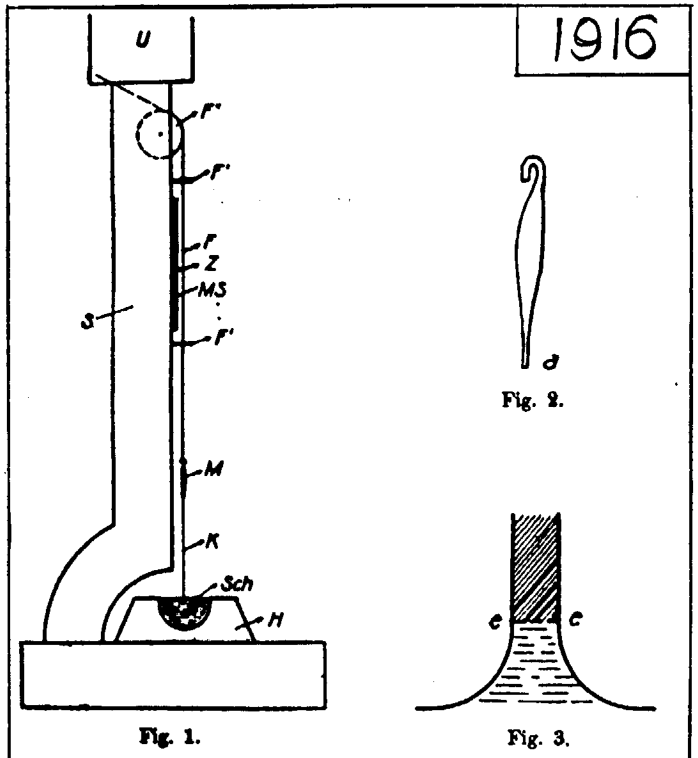

Fig. 1. Fig. 2. Fig. 3.

FIG. 4 - DIAGRAM OF THE MEASUREMENT OF CRYSTALLIZATION RATE OF METALS

Silicon + Germanium
Teal + Little (1949)

Oxides
Nassau + Broyer (1962)

# Meniscus-Controlled Growth

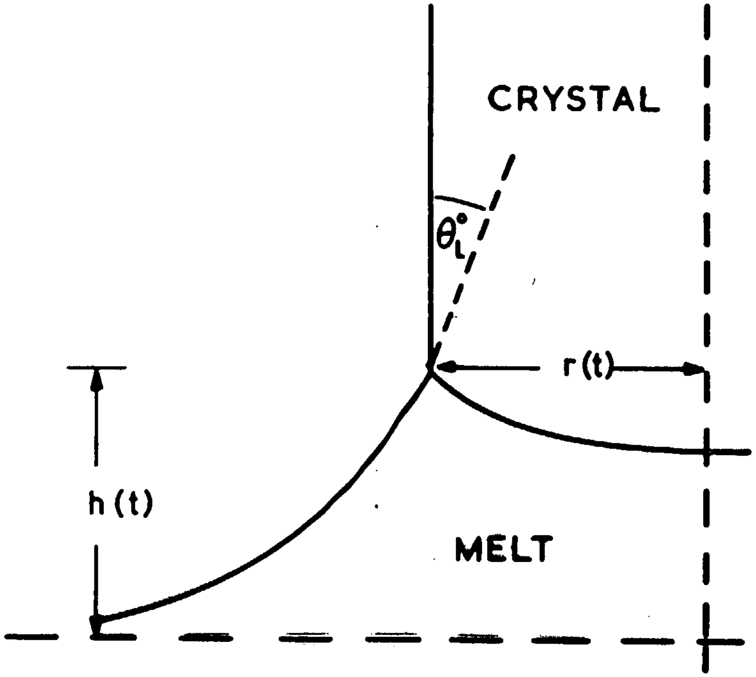

| Material | Contact angle ($\Theta_L^0$)(degrees) |
|---|---|
| Ge | 13 ± 1 |
| Si | 11 ± 1 |
| Cu | 0 |
| $LiNbO_3$ | 0 |
| LiF | 19 |
| $Al_2O_3$ | 17 ± 4 |

# Growth Interface Shape Effects

**Both effects lead to impurity and defect incorporation**

## Faceting

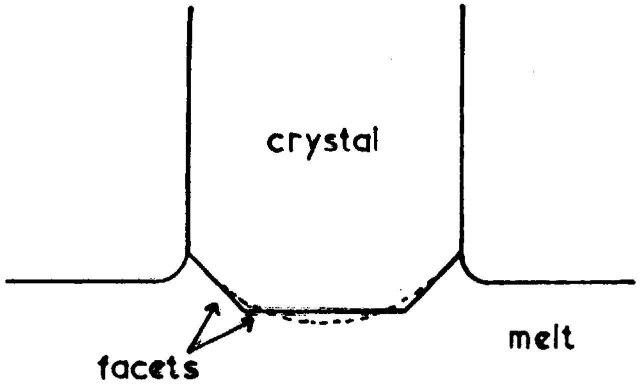

## Curvature

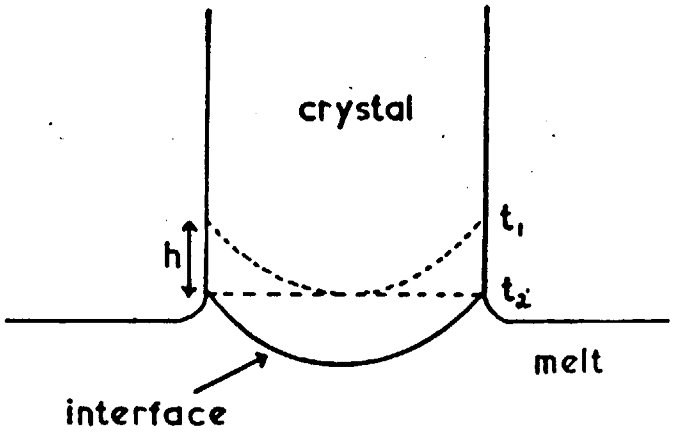

# Cz-Oxide Growth Conditions

| Compound | Melting point (°C) | Crucible material | Atmosphere | Pulling rate (mm h$^{-1}$) | Rotation rate (rpm) |
|---|---|---|---|---|---|
| $Pb_5Ge_3O_{11}$ | 738 | Au | $O_2$ | 1–10 | 10–20 |
| $Bi_{12}GeO_{20}$ | 930 | Pt | $O_2$ | 5–15 | 10–50 |
| $PbMoO_4$ | 1070 | Pt | $O_2$ | 1–10 | 10–40 |
| $ZnWO_4$ | 1200 | Pt | air | 5–15 | 5–50 |
| $LiNbO_3$ | 1250 | Pt | $O_2$ | 5–10 | 5–40 |
| $Sr_xBa_{1-x}Nb_2O_6$ | 1400 | Pt | $O_2$ | 1–10 | 10–20 |
| $Ba_2NaNb_5O_{15}$ | 1450 | Pt | $O_2$ | 1–10 | 10–20 |
| $CaWO_4$ | 1600 | Ir | $A/O_2$ or $N_2/O_2$ | 1–10 | 5–40 |
| $LiTaO_3$ | 1650 | Ir | $A/O_2$ or $N_2/O_2$ | 5–10 | 5–40 |
| $Gd_3Ga_5O_{12}$ | 1825 | Ir | $A/O_2$ or $N_2/O_2$ | 1–10 | 10–100 |
| $YAlO_3$ | 1870 | Ir | $A/O_2$ or $N_2/O_2$ | 1–10 | 10–20 |
| $Gd_3Sc_2Ga_5O_{12}$ | 1875 | Ir | $A/O_2$ or $N_2/O_2$ | 1–10 | 10–20 |
| $Y_3Al_5O_{12}$ | 1970 | Ir | $A/O_2$ or $N_2/O_2$ | 1–10 | 10–20 |
| $Al_2O_3$ | 2105 | Ir | A or $N_2$ | 1–10 | 10–20 |
| $MgAl_2O_4$ | 2150 | Ir | A or $N_2$ | 1–10 | 10–20 |

# Rotation in Cz-Grown Oxides

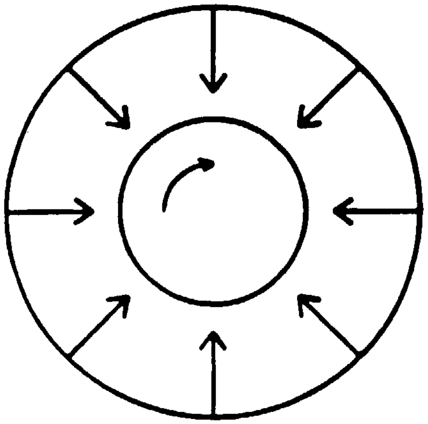

Type I

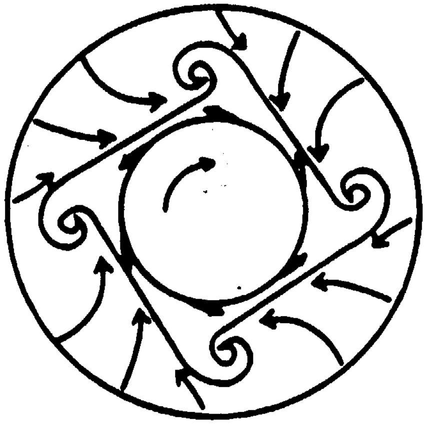

Type II

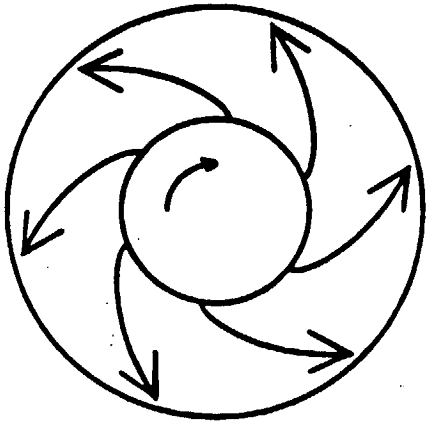

Type III

Fig.5 Section of a short 52 mm diameter Nd:YAG between crossed polarizers showing the termination of the core at the flattening transition.

# Rotational Striations in SBN

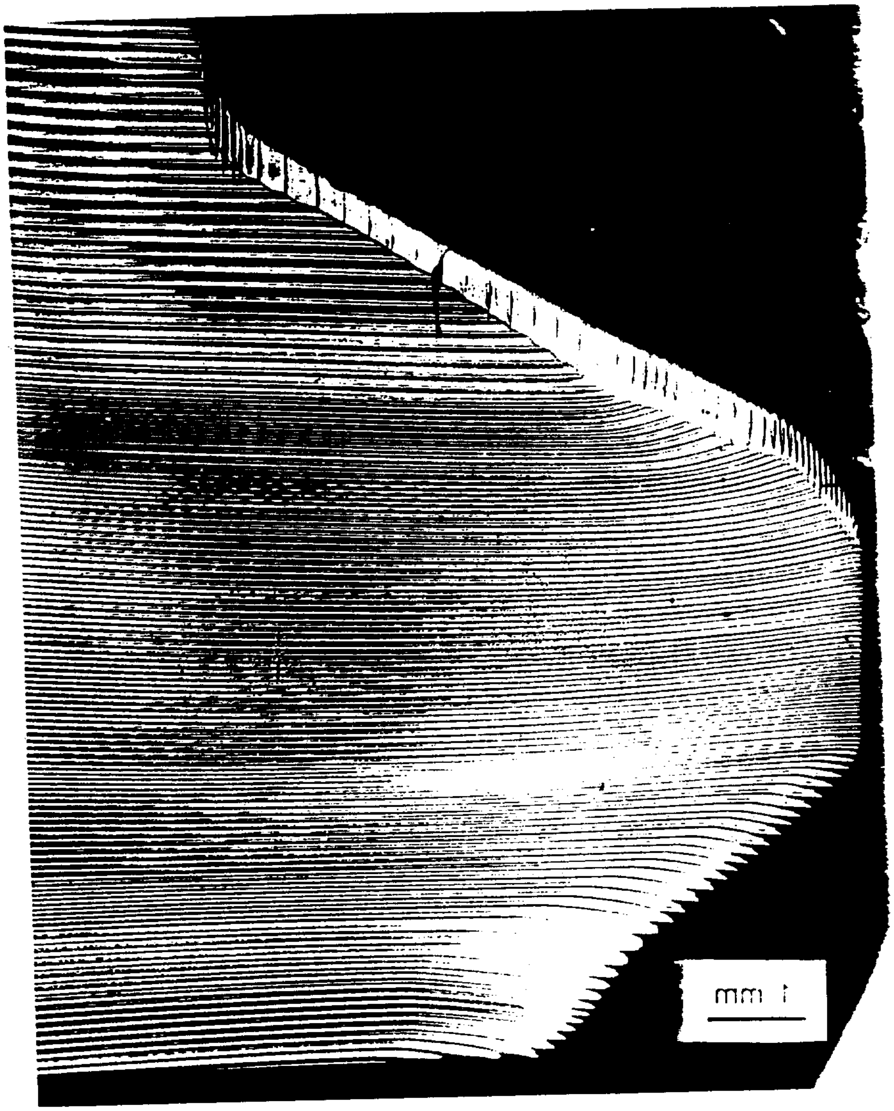

Fig. 2. Longitudinal cross-section of a manually grown boule in a region of changing diameter. The slice was cut perpendicular to a {100} facet plane. The photograph was taken with polarized light in transmission to enhance the viewing of the striations. Both facet and rotational striations are evident.

# Sapphire

**Line compound melting congruently**
**Grows readily by a variety of techniques**

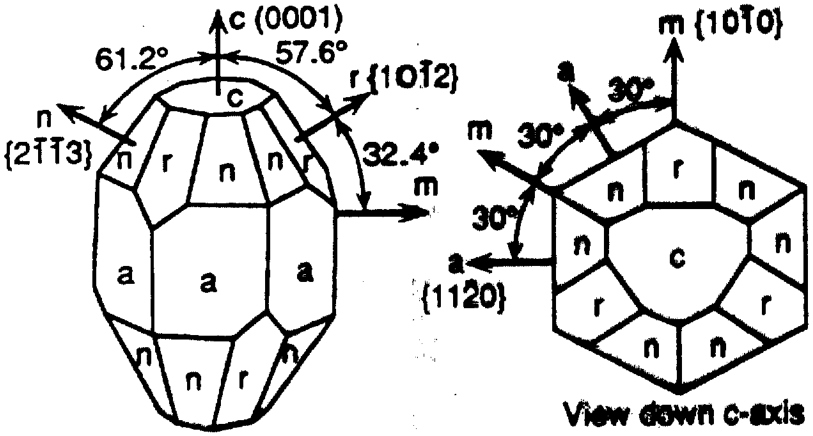

Figure 1. Sapphire ($\alpha$-$Al_2O_3$) crystal showing mineralogical and Miller index notation.

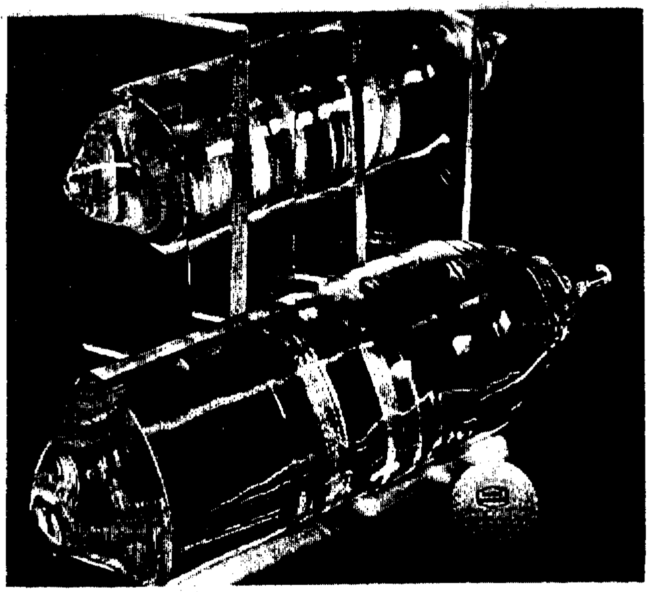

*Four-Inch Diameter Sapphire Boule Showing Semi-finished Polished Plates Cut From the Crystal.*

# Cz Sapphire Boules

**Union Carbide Crystal Products**
**R-plane to 6 " dia x 6 " long**
**a-axis and c-axis to about 4 " dia.**

# Czochralski Crystal Growth Station

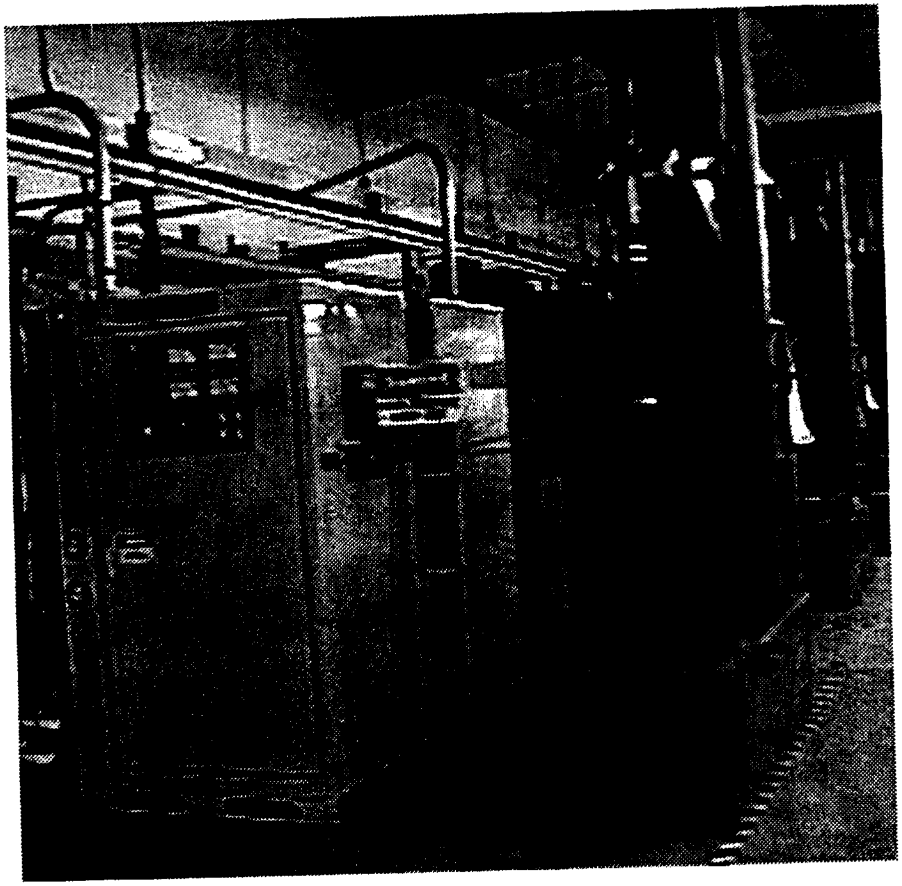

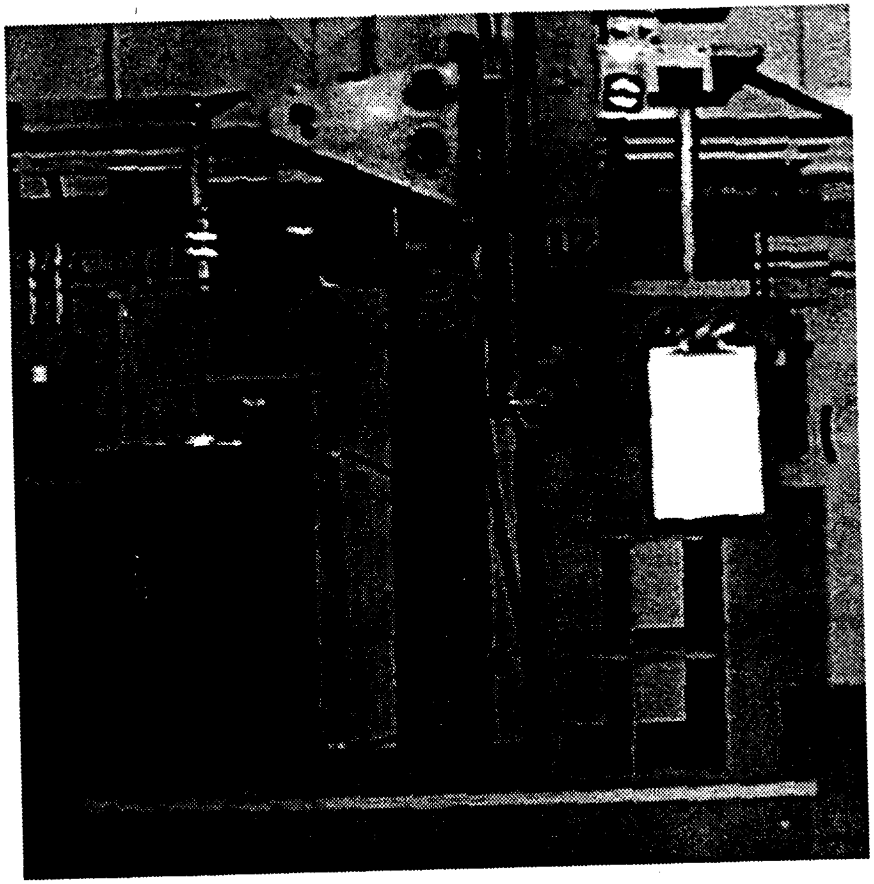

# Defects in Sapphire

## Caused by excessive stress in neck of boule

Fig. 6. X-ray topograph of dislocation tangles in sapphire single crystal. Note a formation of low-angle grain boundaries. Ag $K_{\alpha 1}$ radiation.

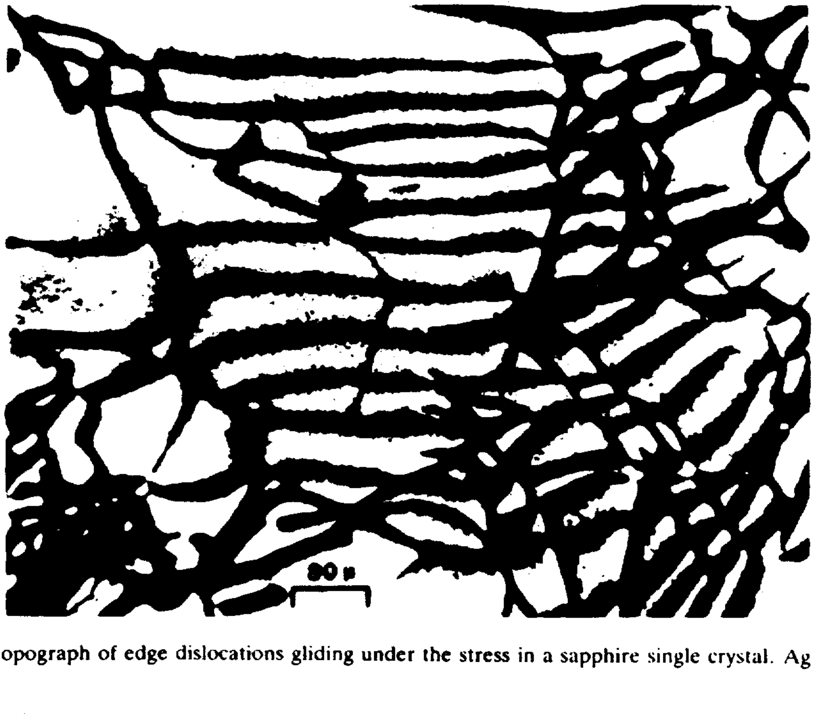

Fig. 7. X-ray topograph of edge dislocations gliding under the stress in a sapphire single crystal. Ag $K_{\alpha 1}$ radiation.

# Kyropoulus Growth Method

Little or no pulling, depending on $\rho_l/\rho_s$

Effective with sapphire using moly crucibles

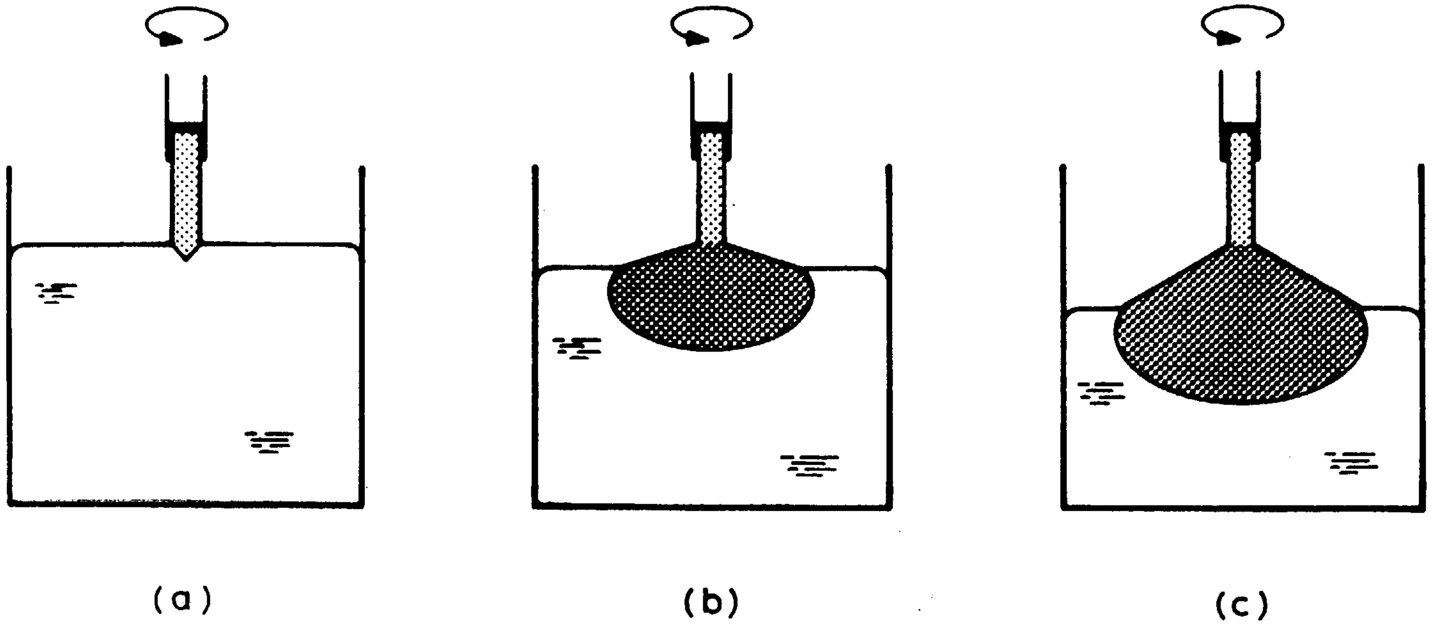

**Figure 4.4** The sequence used in Kyropoulos growth. (*a*) The pointed seed crystal is brought into contact with the melt. A small amount of seed is melted and then cooling is commenced to give the situations (*b*) and (*c*). Note that the shape grown depends quite strongly on the temperature distribution and the relative densities of the melt and crystal.

# Kyropoulus Sapphire

## S&R Rubicon, sizes to 12 " ϕ

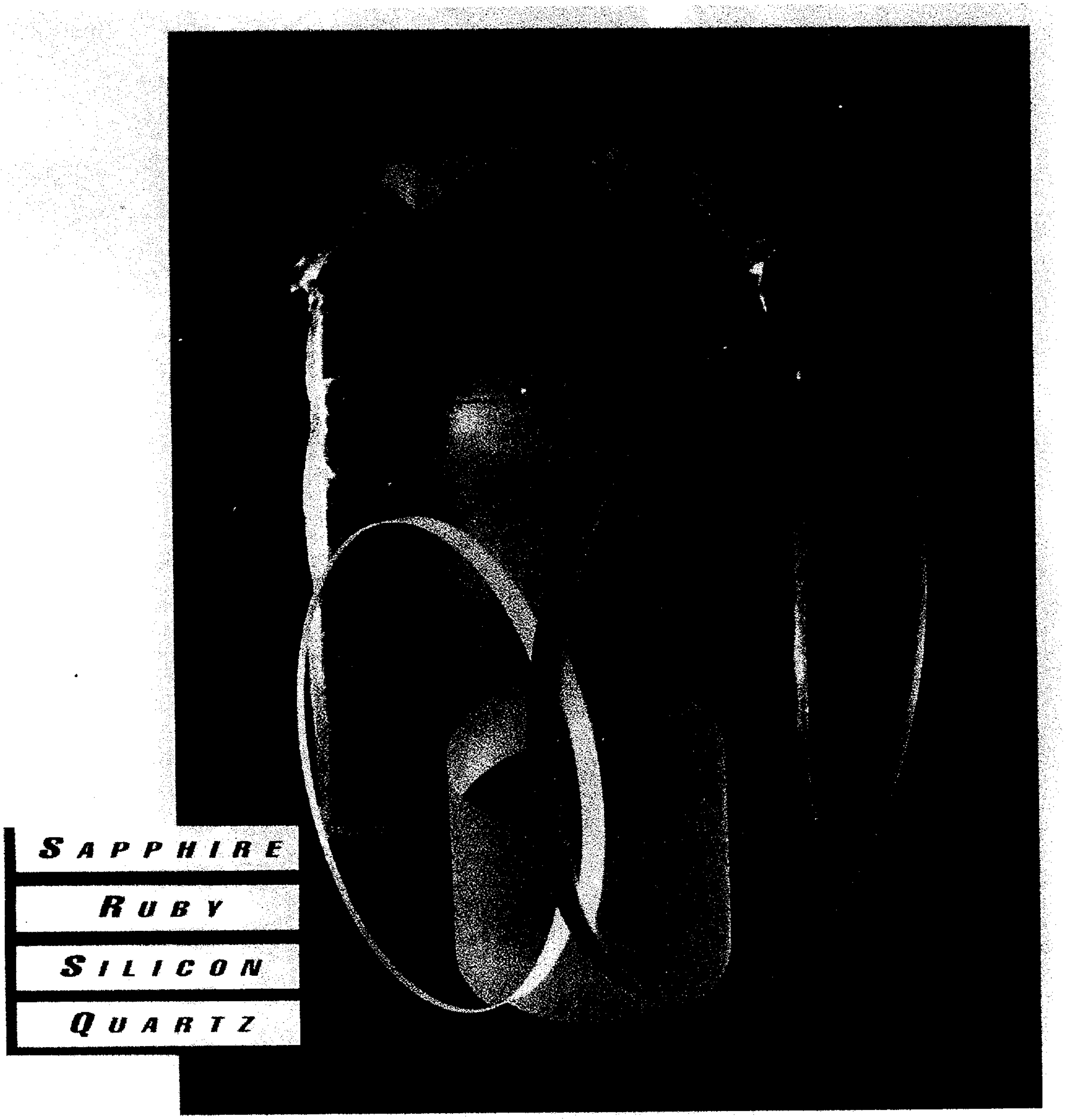

# HEM Growth Technique

1970

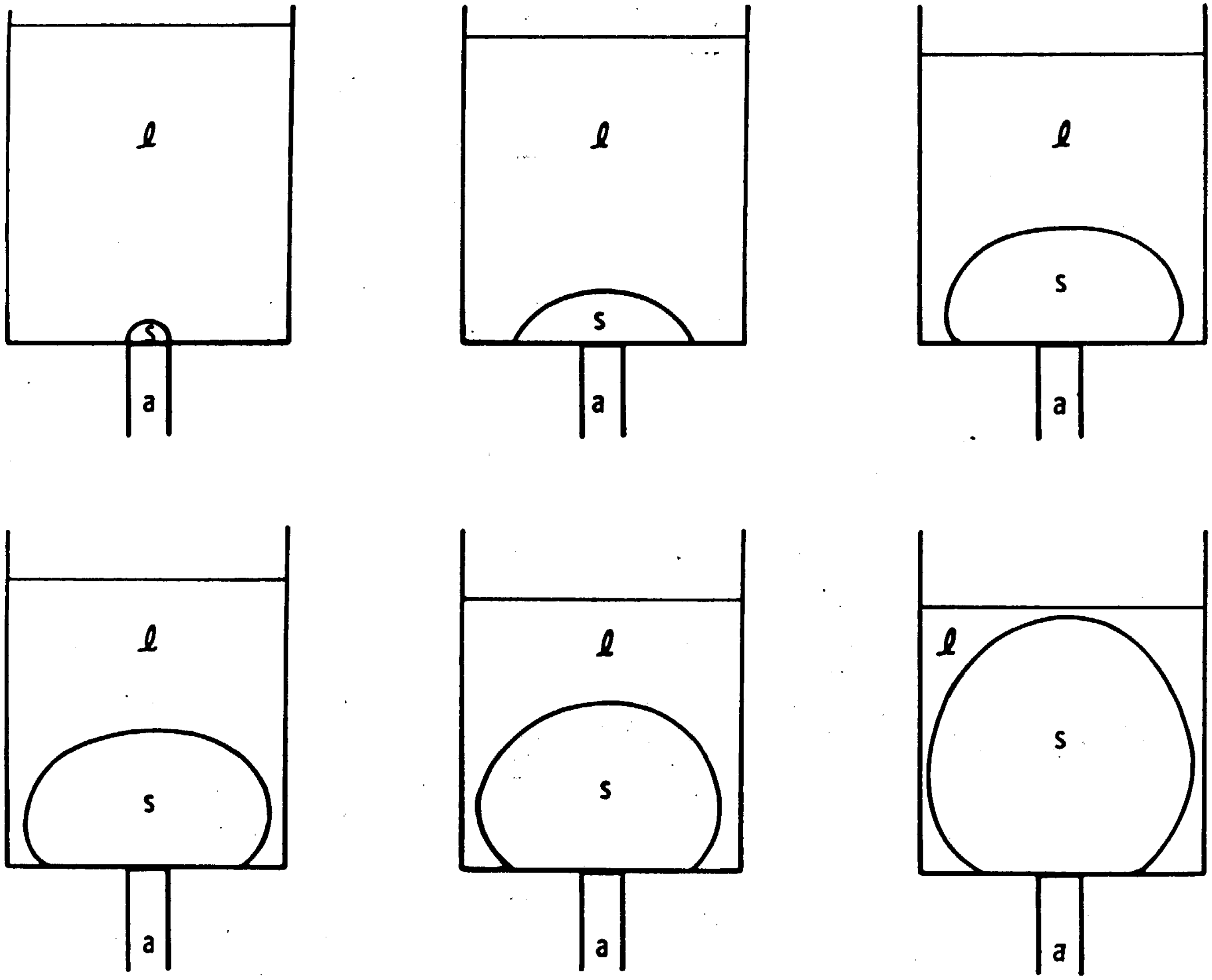

# HEM Growth System

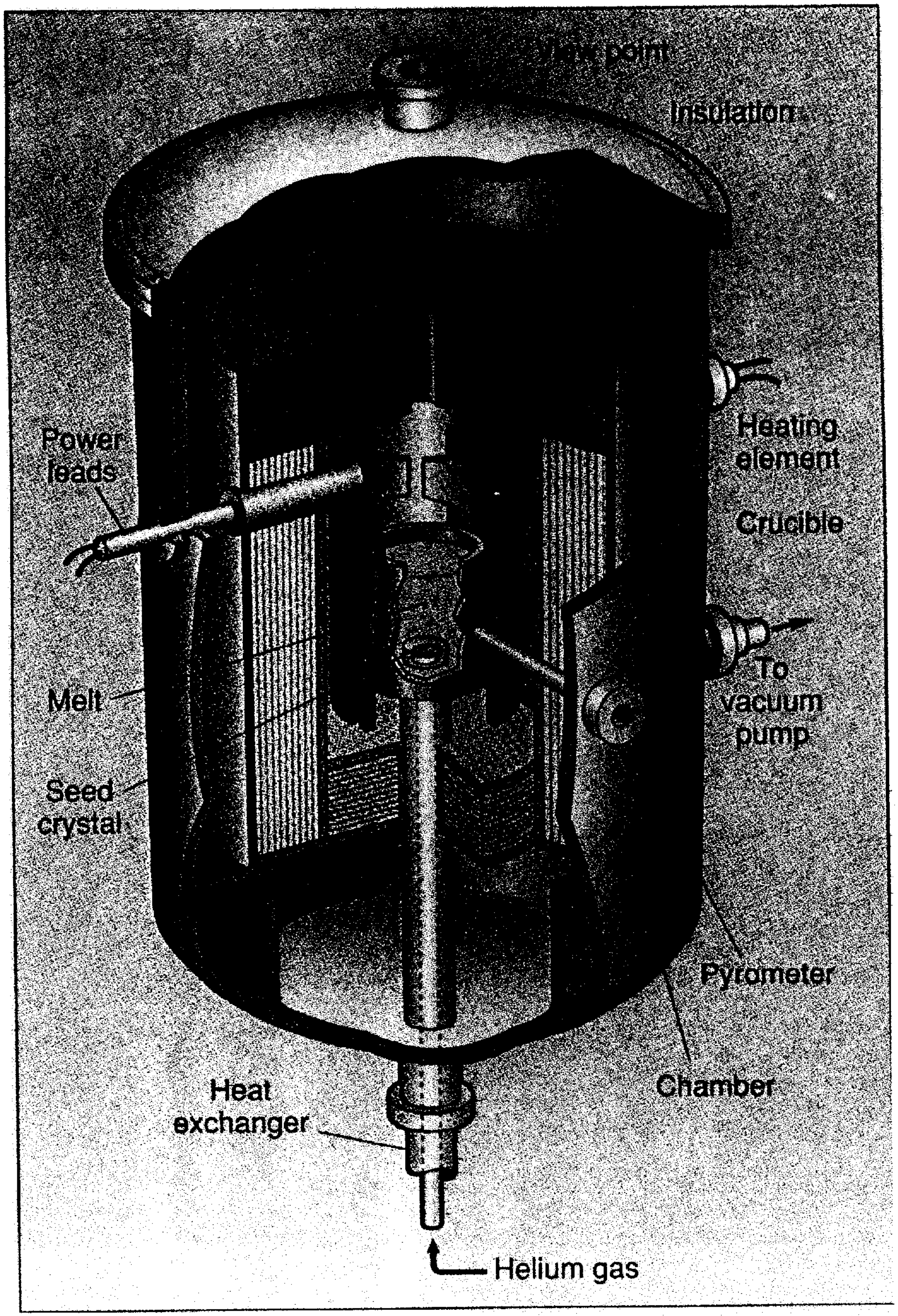

# Growth Interface - HEM Sapphire

Crystal Systems, Inc.

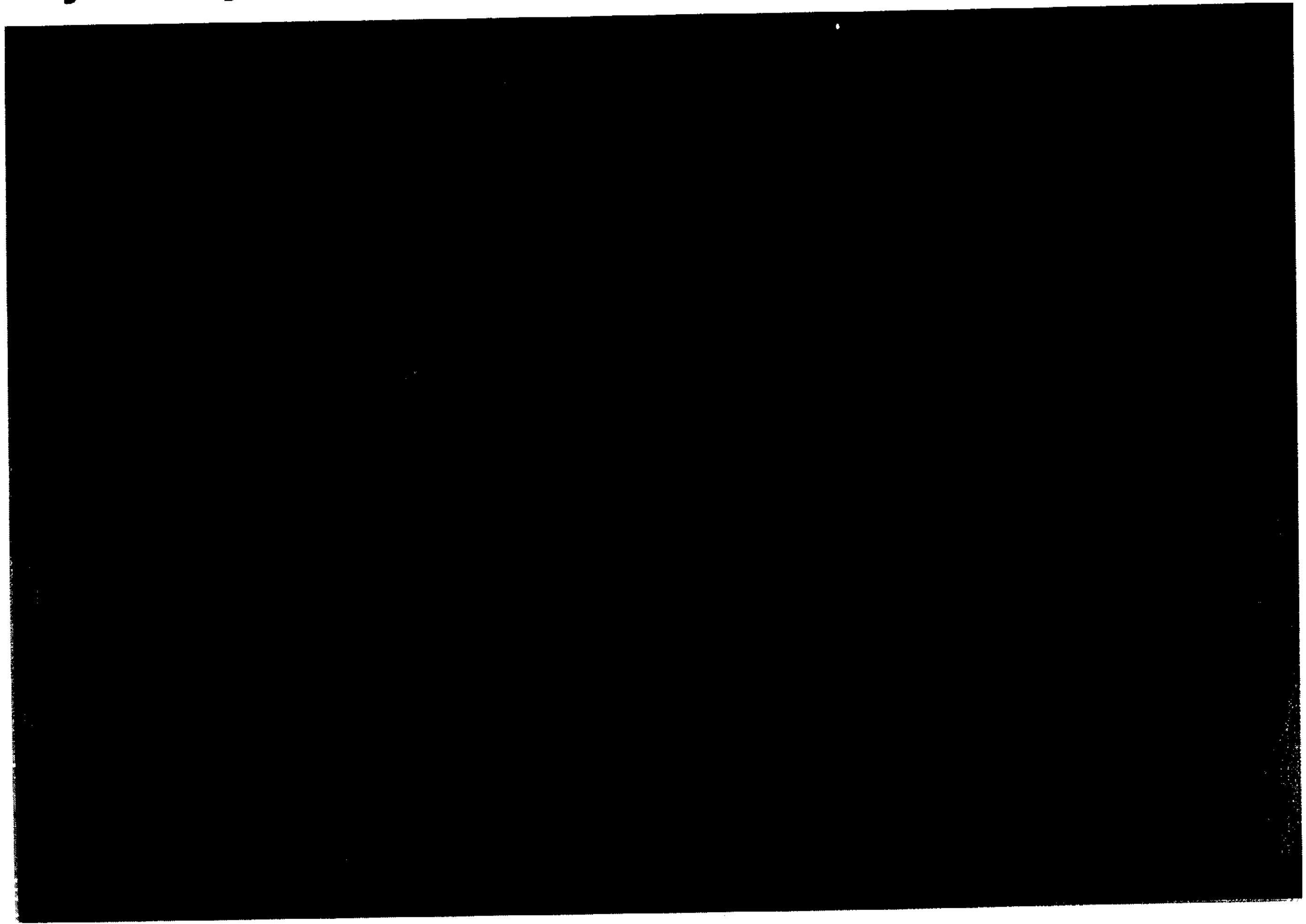

# HEM Sapphire Ingot

## a-axis orientation, 6-8*-11-13 " $\phi$

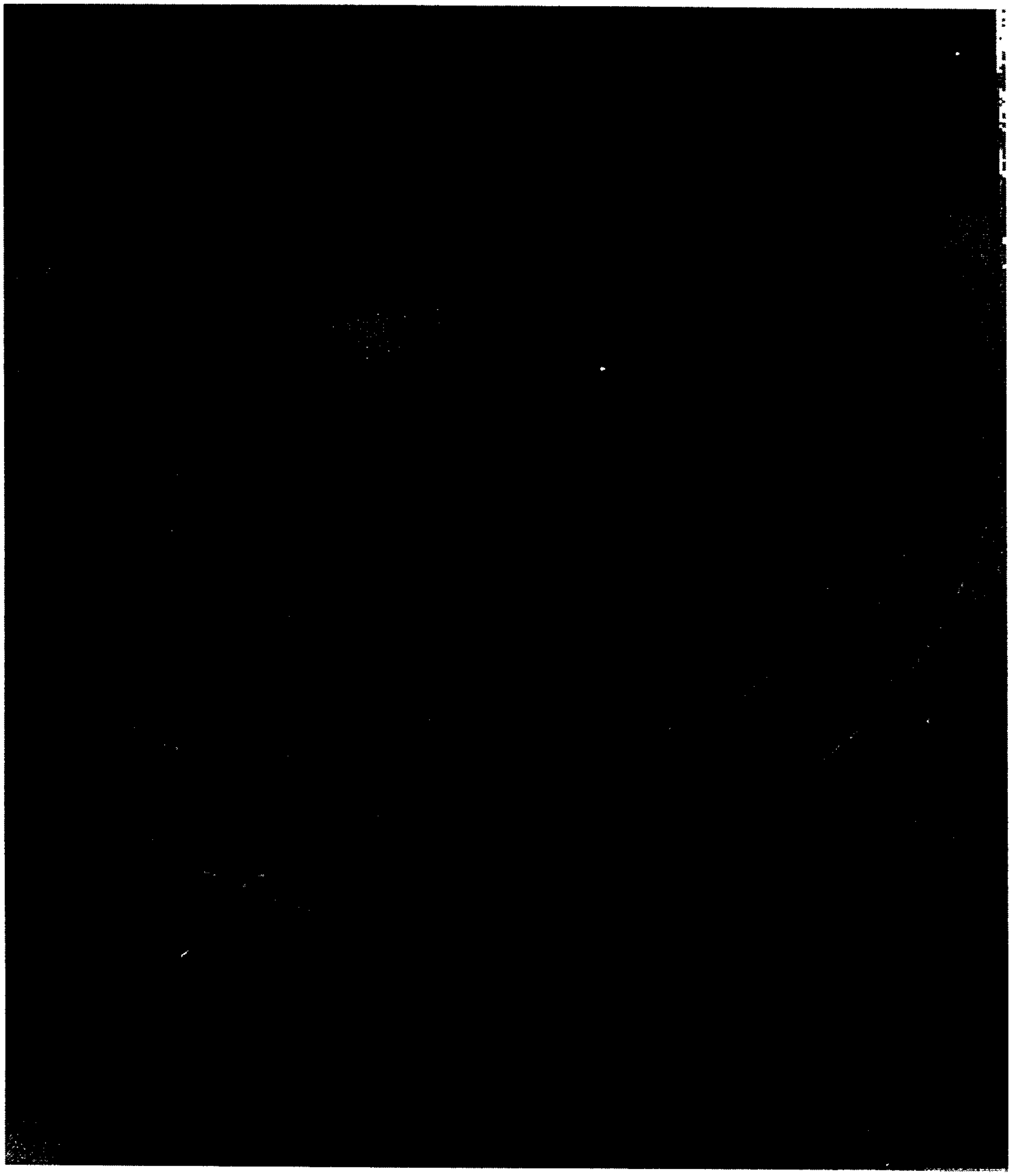

# A-axis cores - HEM Sapphire

## Crystal Systems, Inc.

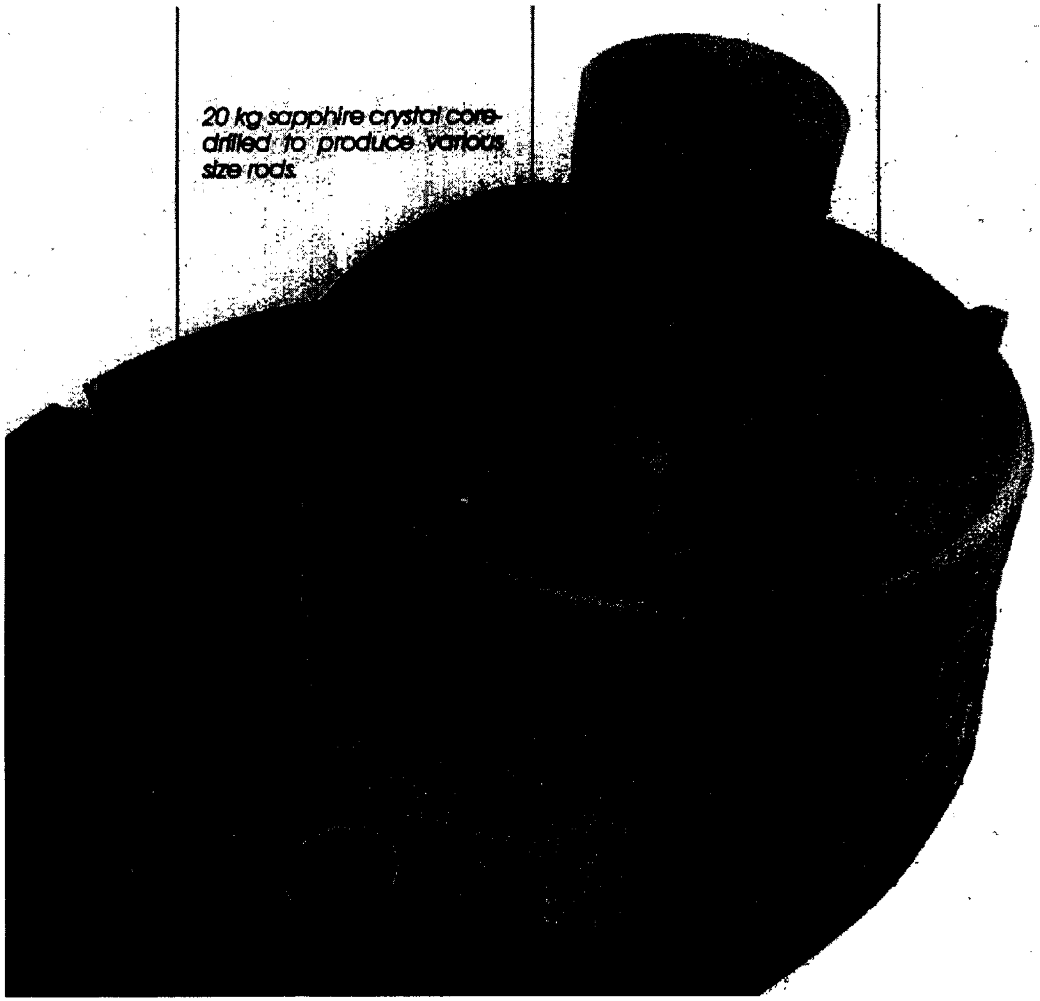

20 kg sapphire crystal core-drilled to produce various size rods.

# C-axis cores - HEM Sapphire

## Crystal Systems, Inc.

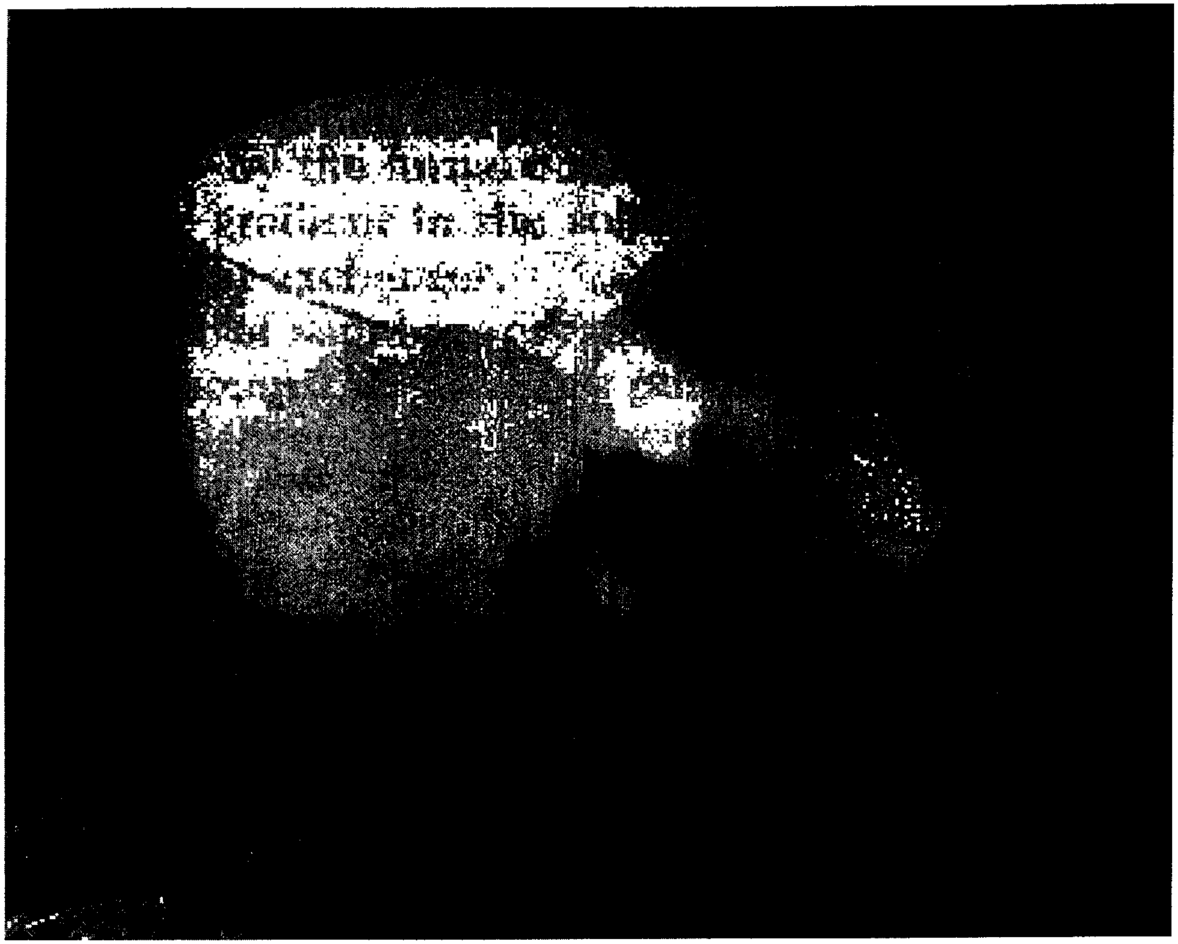

# Commercial Sapphire Windows

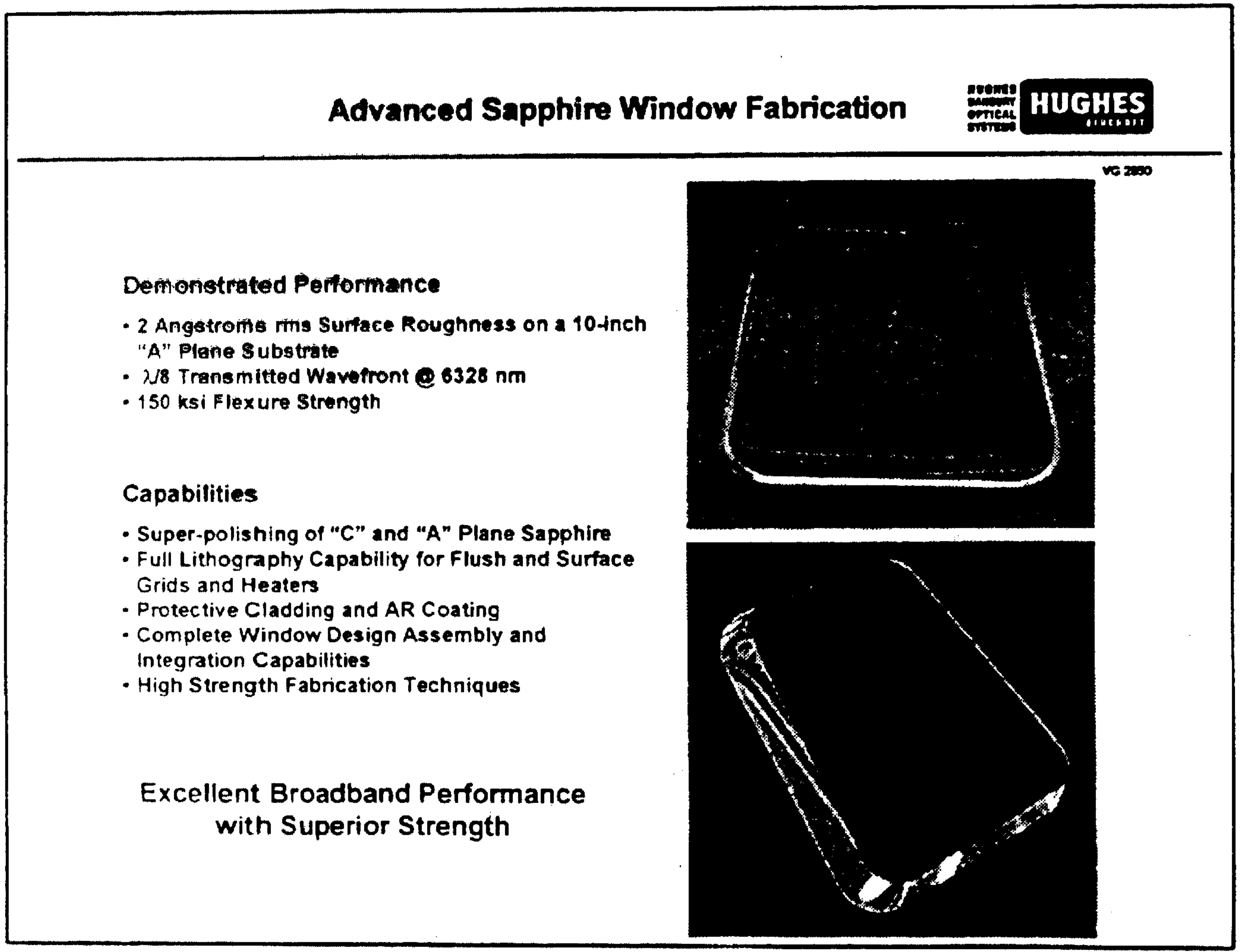

## Advanced Sapphire Window Fabrication

VG 2850

**Demonstrated Performance**

- 2 Angstroms rms Surface Roughness on a 10-inch "A" Plane Substrate
- λ/8 Transmitted Wavefront @ 6328 nm
- 150 ksi Flexure Strength

**Capabilities**

- Super-polishing of "C" and "A" Plane Sapphire
- Full Lithography Capability for Flush and Surface Grids and Heaters
- Protective Cladding and AR Coating
- Complete Window Design Assembly and Integration Capabilities
- High Strength Fabrication Techniques

Excellent Broadband Performance
with Superior Strength

# Commercial Sapphire Windows

## Capabilities Summary

VG 2850A

- Developed High Performance Sapphire Windows Integrating:
    - Superpolishing Processes Providing:
        - RMS Transmitted Wavefront Error:
            - Conventional Processes: <<0.125 Wave
            - Advanced Processes: <0.025 Wave
        - RMS Surface Flatness: <0.2 Wave
        - High Residual Strength/Reduced Subsurface Damage
            - 150 Ksi, 40/20 Scratch/Dig
        - Supersmooth Surfaces – <1 Angstrom RMS
        - Near Zero Wedge Error
    - Post-Polishing Processes for Additional 30% Strength Increase
    - Protected EMI/EMC and Deicing Grid Structures (Flush Grids and Claddings)
    - Transmittance Optimized, Durable Anti-Reflection Coatings
- Currently Producing Windows to 11 Inch Aperture

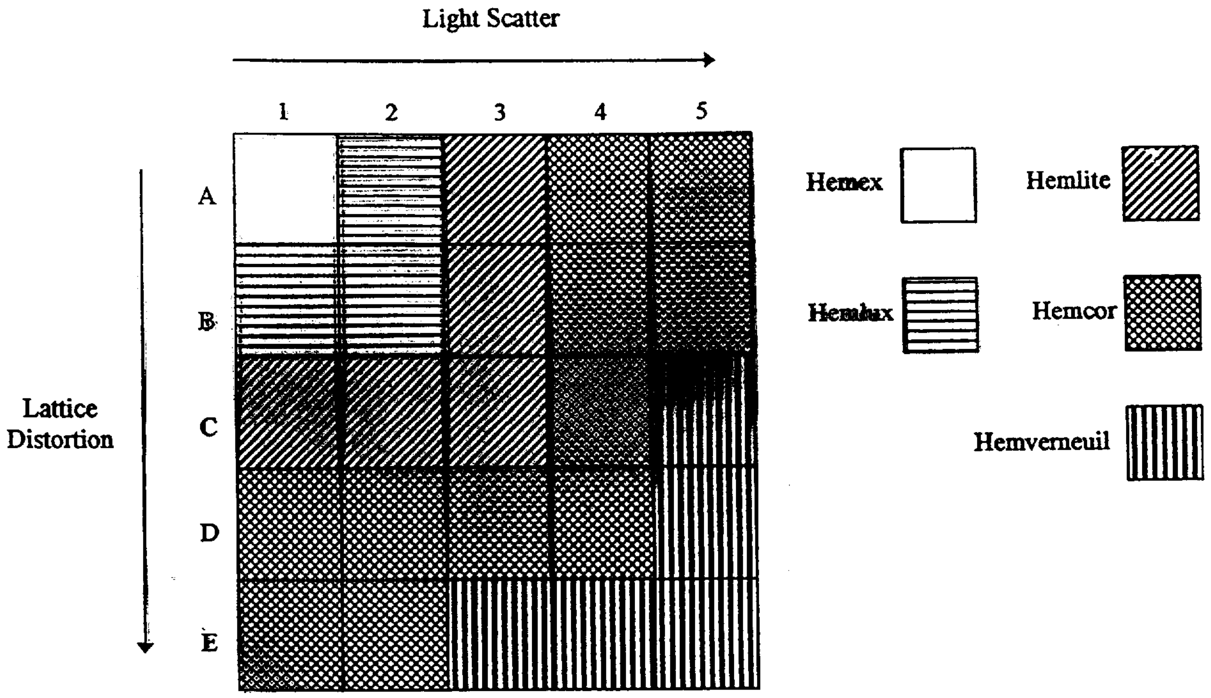

Figure 2. Representation of lattice distortion and light scatter in various grades of sapphire

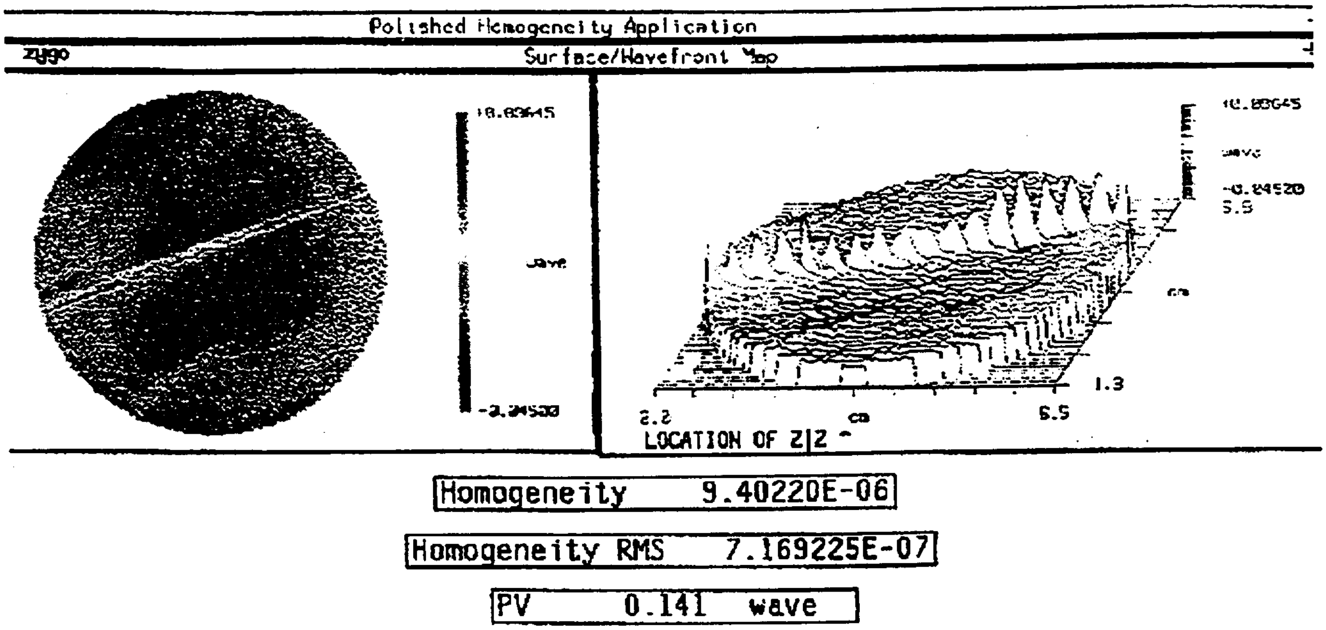

Homogeneity 9.40220E-06

Homogeneity RMS 7.169225E-07

PV 0.141 wave

Figure 4. Refractive index homegeneity for a Hemverneuil grade sapphire with a severe lattice distortion across the sample

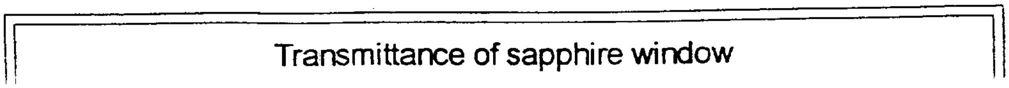

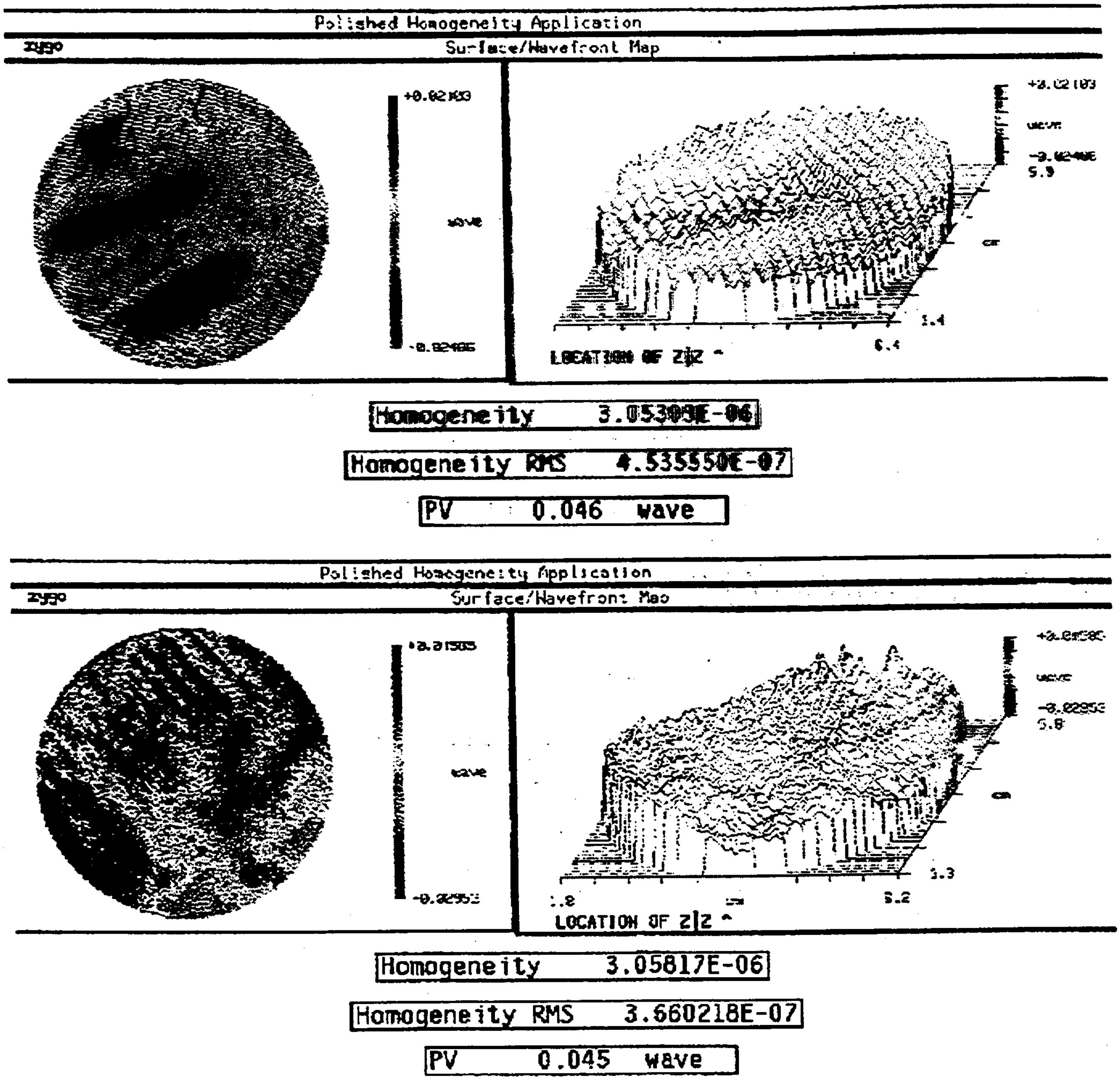

```
Homogeneity        3.05309E-06
Homogeneity RMS    4.535550E-07
PV          0.046   wave
```

```
Homogeneity        3.05817E-06
Homogeneity RMS    3.660218E-07
PV          0.045   wave
```

Figure 3. Refractive index homogeneity of Hemlite grade sapphire with $(11\bar{2}0)$ (above) and (0001) (below) orientations

# Commercial Sapphire

- **Czochralski**
  - Diameters to 6"
  - c-axis, a-axis, R-plane, etc.
  - High optical quality
- **HEM** (Crystal Systems, Inc.)
  - Diameters 6", 8", 11", 13", 20" (in development), heights about 5-6"
  - Growth direction along a-axis (optic axis in plane)
  - High optical quality (best grade HEM)
  - A-plane windows figured to $\lambda/40$ (Hughes/Danbury)
- **Kyropoulus (S&R Rubicon)**
  - Diameters to 12"
  - Optical losses uncertain

# Phase Equlibria in $Y_2O_3$-$Al_2O_3$

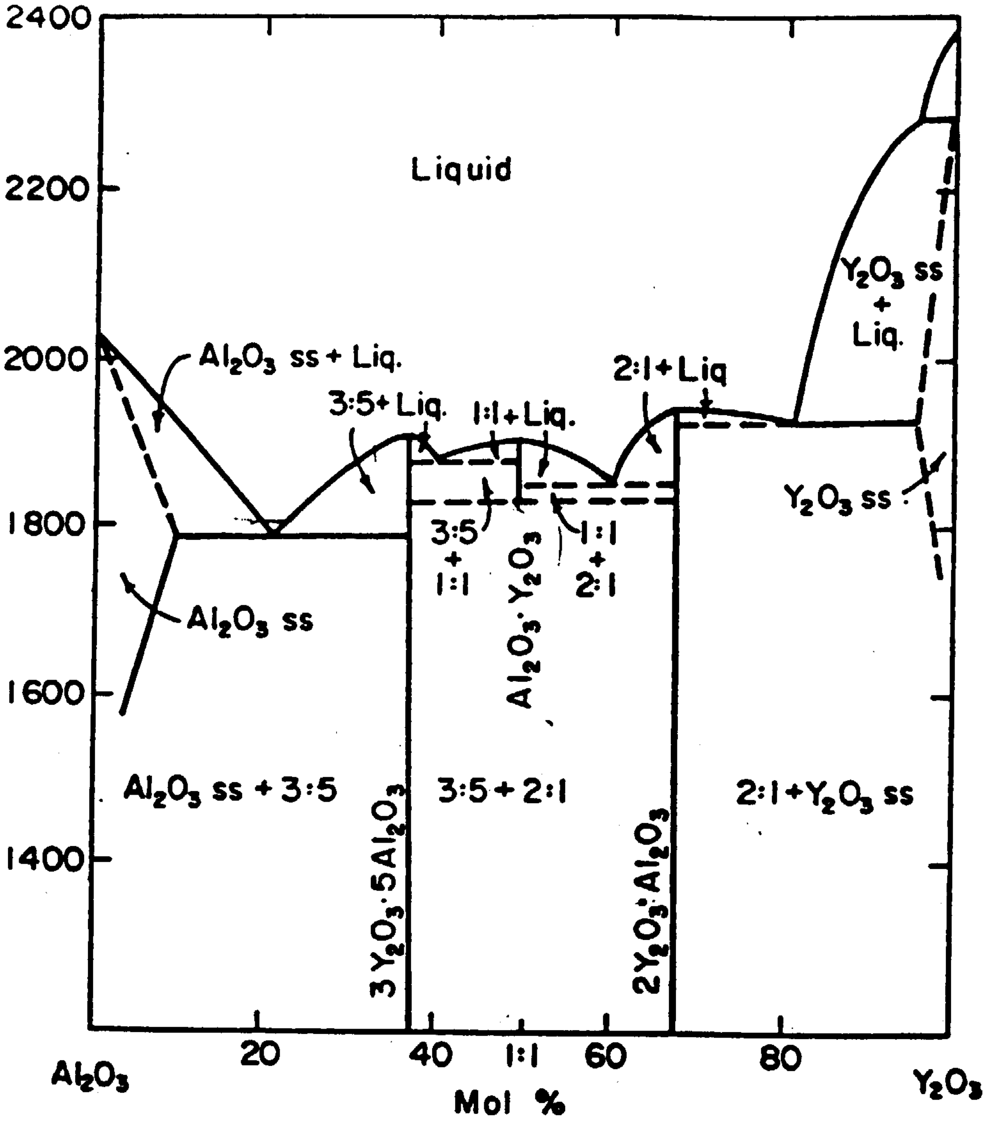

YAG = $Y_3Al_5O_{12}$

# Distortion in Cz-Grown YAG

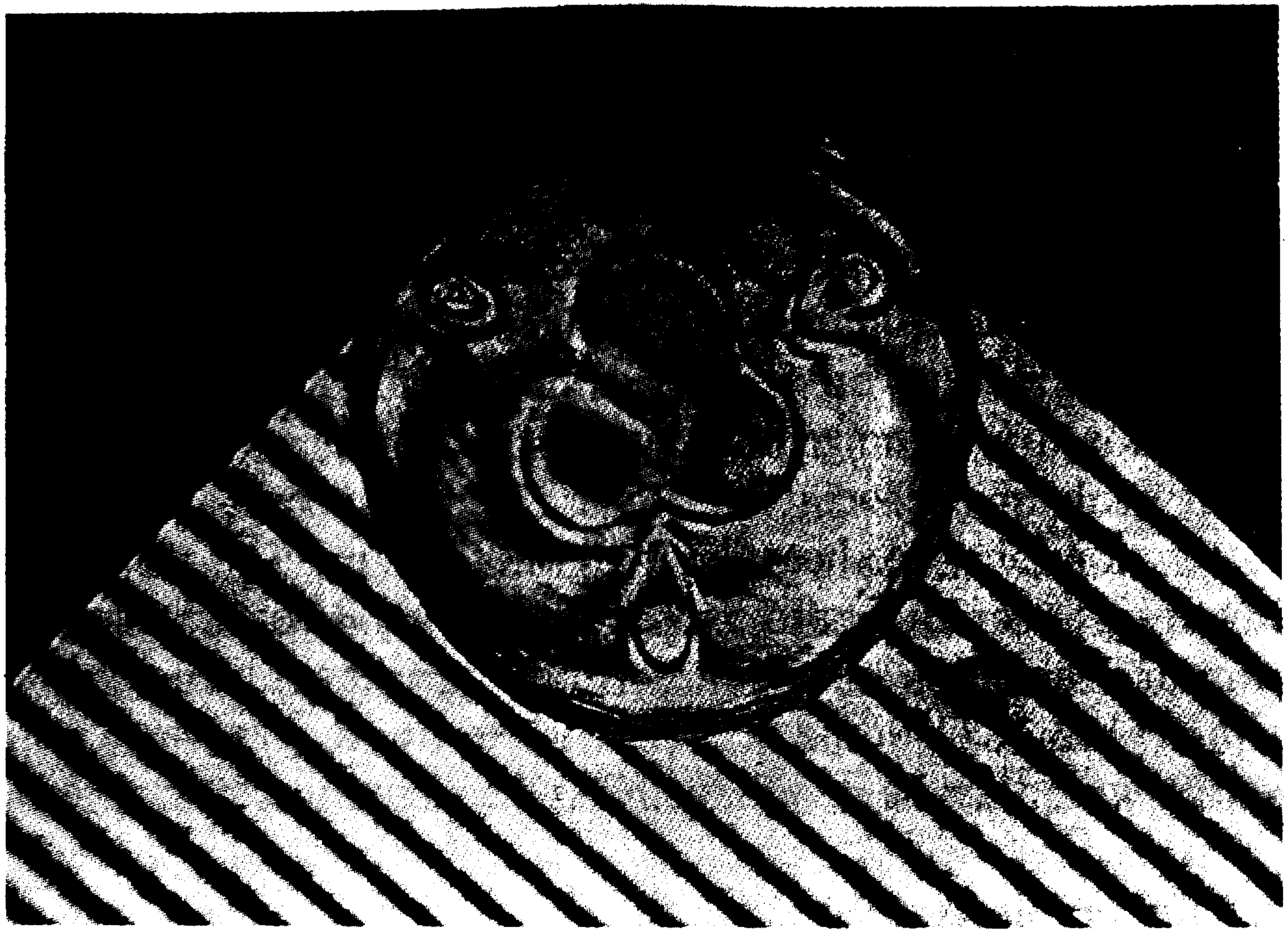

Fig. 55. The strain pattern observed along the ⟨111⟩ axis of a single crystal of $Y_3Al_5O_{12}$ showing clearly the effects induced by three symmetrically placed {211} interface facets near to the crystal centre and a further three {110} interface facets near to the crystal periphery. Mag. × 4.

# Cz Growth Interface Shapes

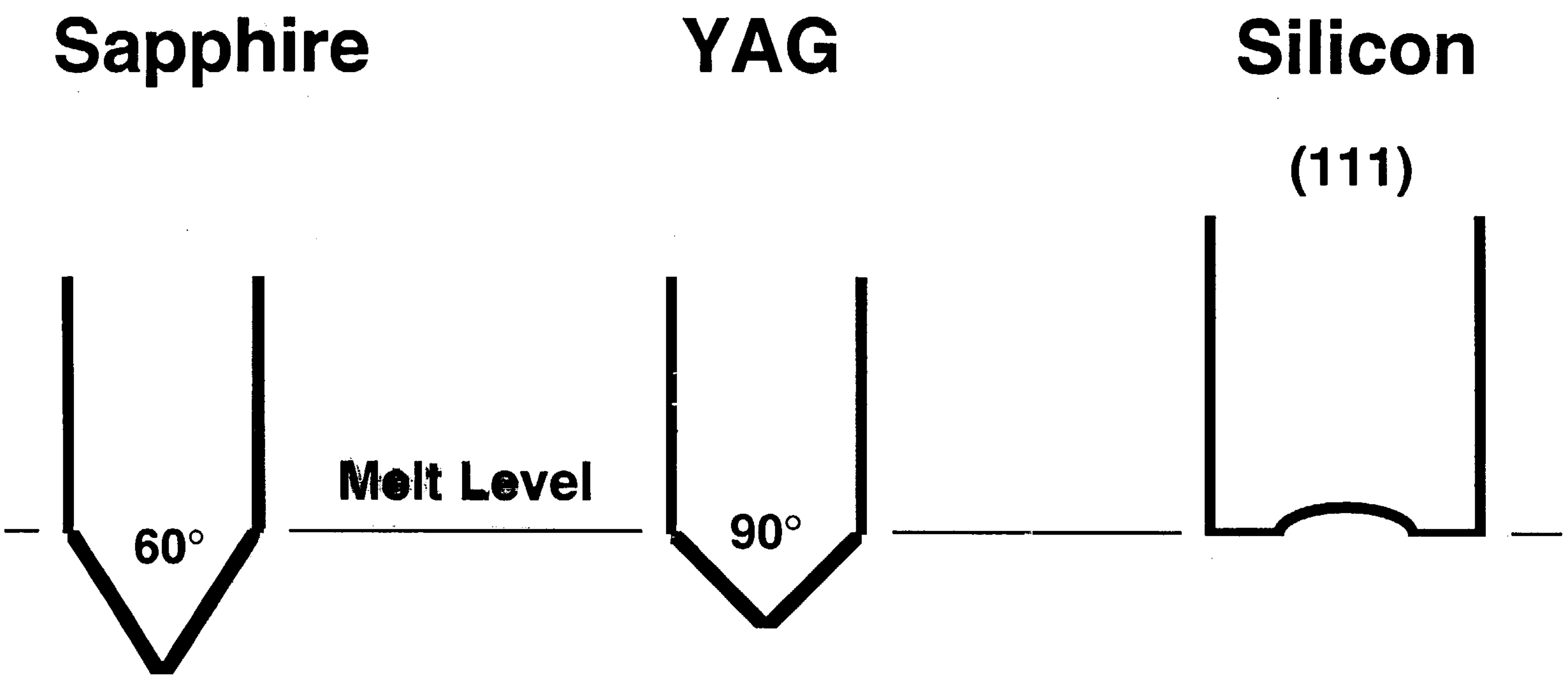

# YAG by HEM Method

**Diameters 3 " and up**
**[100] and [111]**

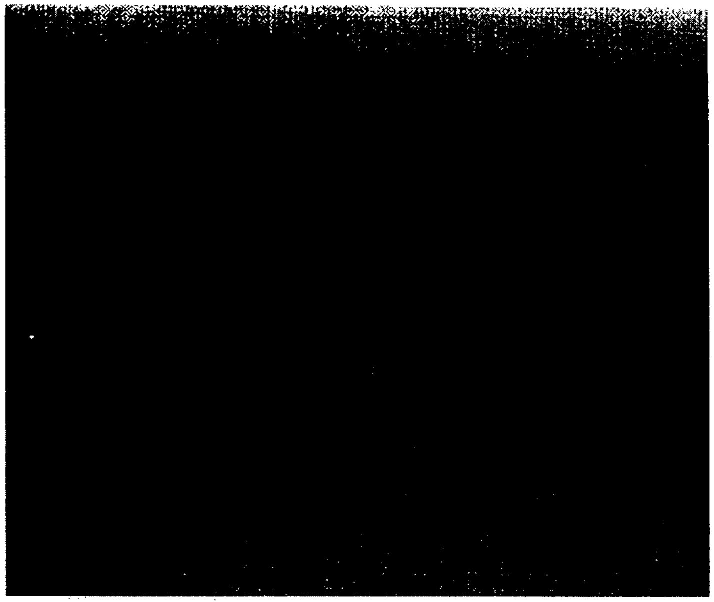

**Domed Interface**

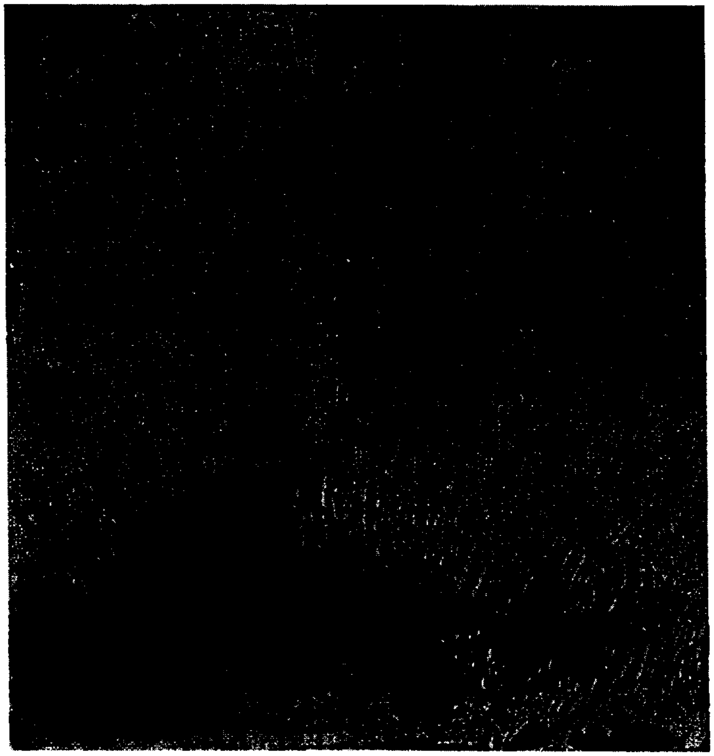

**Flatter Interface**

# Modified HEM Method with Flat Interface

## Birdcage heater to achieve tapered temperature profile

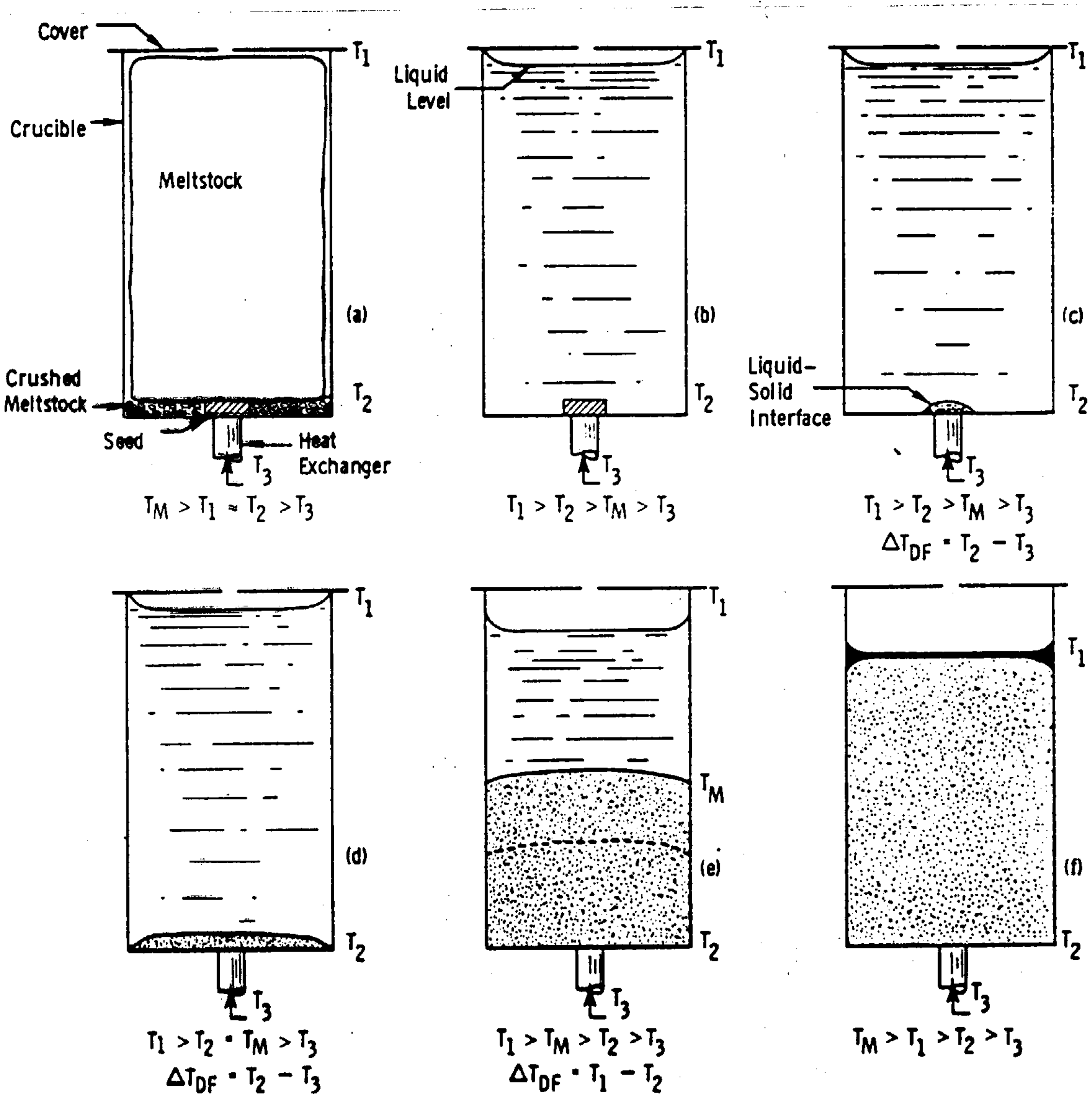

# Graphite HEM Heaters

**Flat Interface** **Domed Interface**

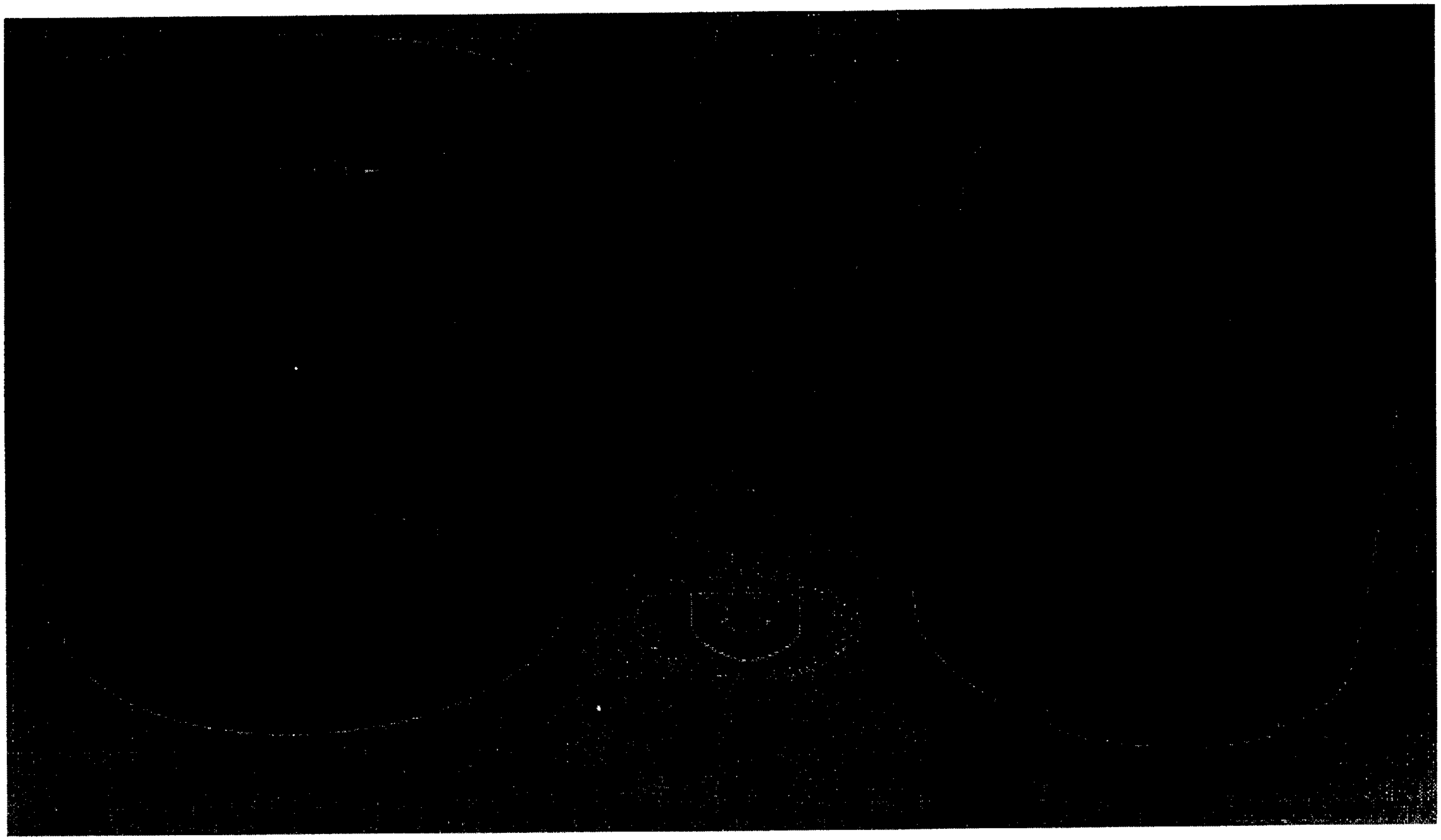

# Growth of YAG by Modified HEM Method having Flat Interface

J. J. Caslavsky and D. Viechnicki
Both undoped and Nd-doped YAG in [100] and [111] orientations
Core-free crystals to 3 " dia x 4.5 " high

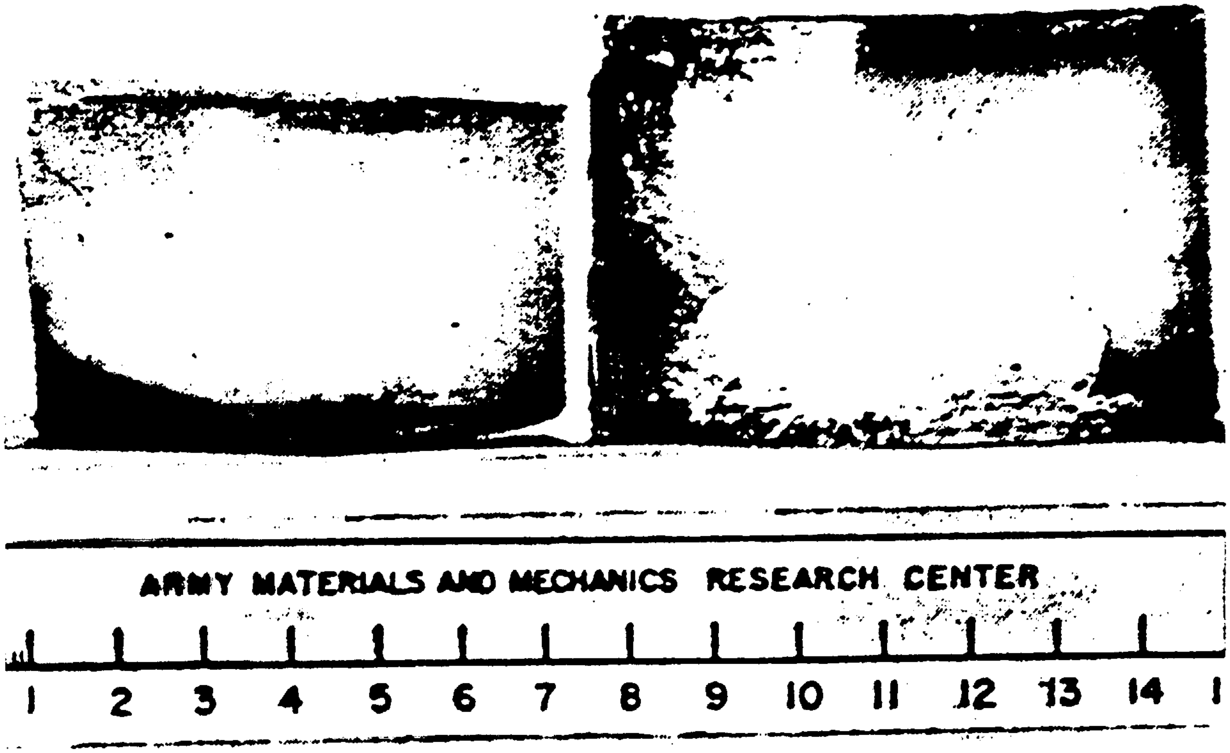

# Growth of YAG by Modified HEM Method having Flat Interface

J. J. Caslavsky and D. Viechnicki
Both undoped and Nd-doped YAG in [100] and [111] orientations
Core-free crystals to 3 " dia x 4.5 " high

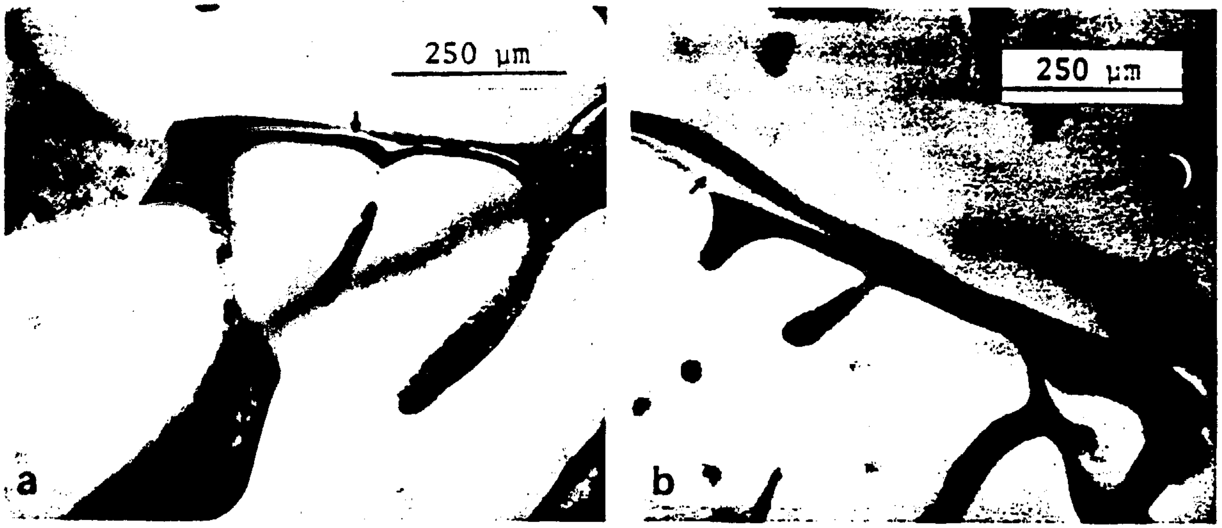

Fig. 4. Optical photomicrographs of second phase inclusions in YAG single crystals. Arrows denote voids in channels containing inclusions formed due to solid–liquid contraction. The second phase liquids solidified after the matrices: (a) $YAlO_3$ inclusion; (b) $Al_2O_3$ inclusion. 280 X.

# YAG by Gradient Freeze - TGT
## (Vertical Bridgman with Flat Interface)

**Shanghai Institute of Fine Mechanics by Yongzong ZHOU**
**Nd-doped at 1.1 At% , 5 cm dia , [111]-axis**
**CORE-FREE**

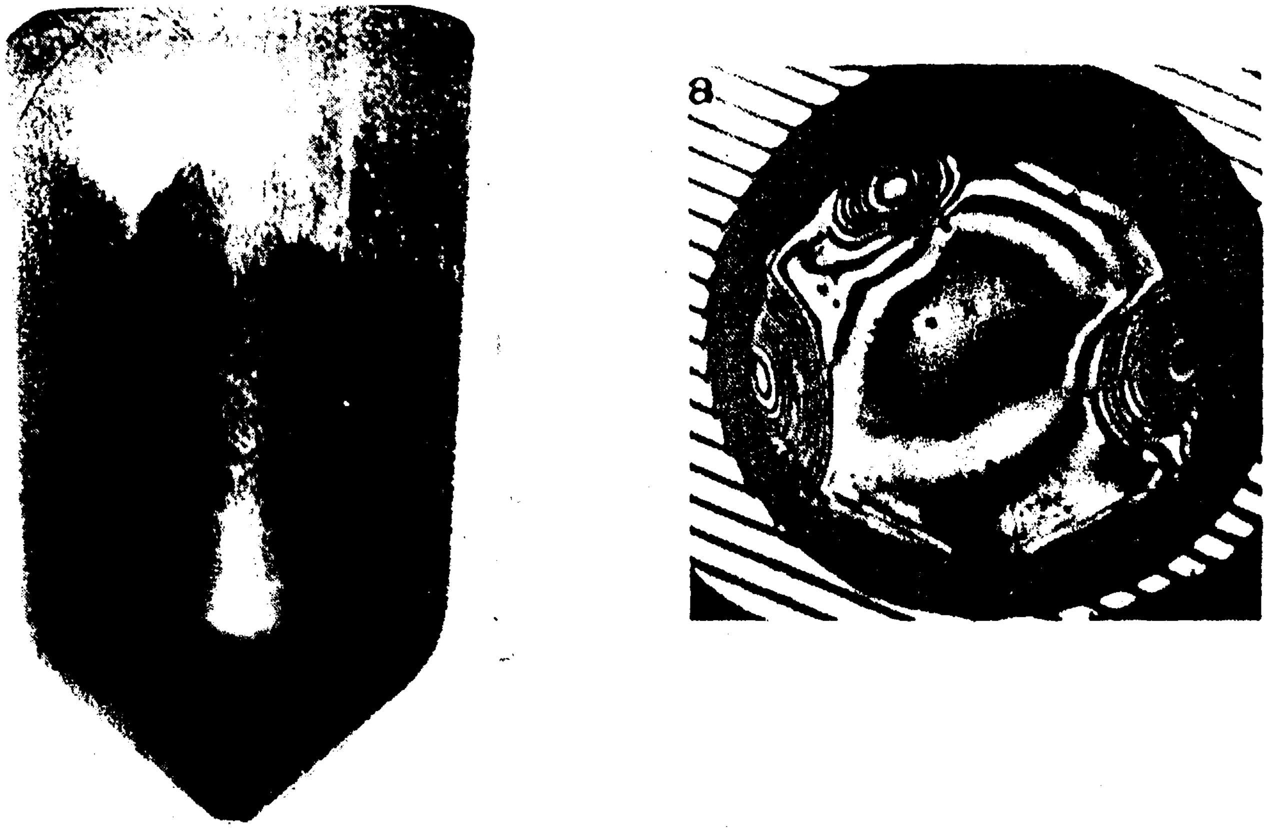

# Silicon Q - Factor Determination

4" Φ x 8" Long
Monsanto Cz
p-type (B-doped)
$2.7 - 4.5 \times 10^{15}$ cm$^3$
3-5 Ω cm
Carbon $8 \times 10^{16}/\text{cm}^3$
Zero-d ($< 10^{-2}$)

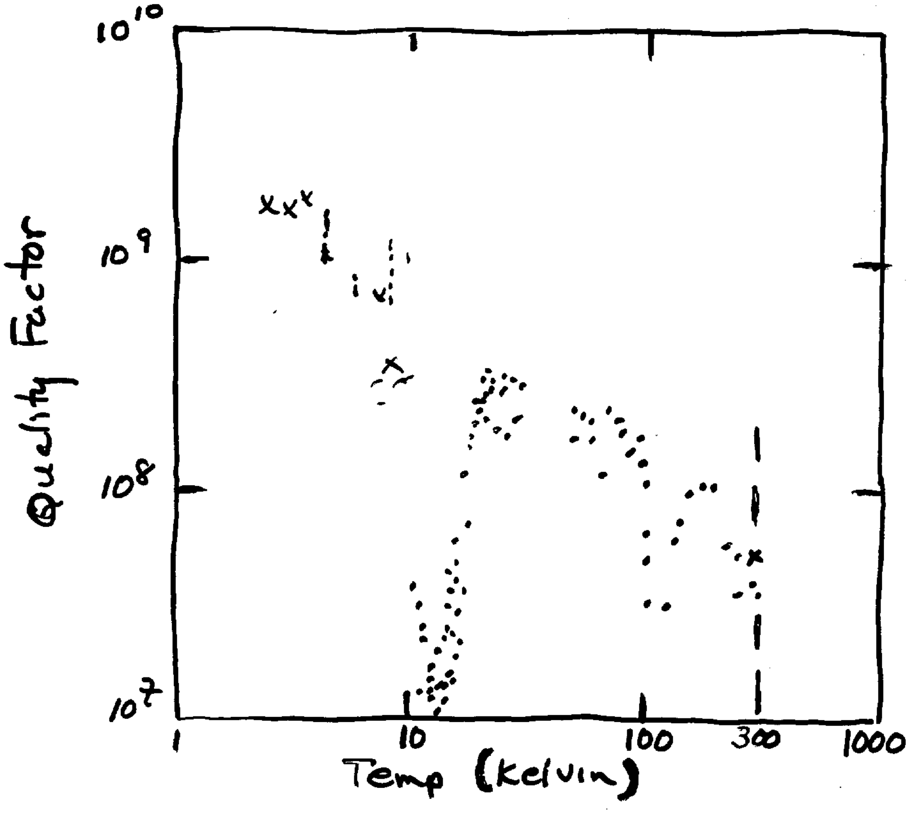

D.F. McGuigan et al
J. Low Temp. Physics 30, 621 (1978).

# Commercial Silicon Capabilities

- **Czochralski**
  - Contains controlled levels of oxygen ($10^{18}$ cm$^{-3}$) originating from $SiO_2$ crucible
  - Used for low-power electronics
  - Up to 22 " Φ (poly)
  - Up to 20 " Φ (zero d.)
  - 12 " Φ (standard in industry, Sematech)
    - » 12 " Φ x 4 "long - $17.5 K
- **Float-Zone**
  - Oxygen "free" (~$10^{14}$ cm$^{-3}$)
  - Used for high power applications
  - 4 "Φ (zero d.)
- **HEM**
  - Polycrystalline, useful for solar cell applications

# Zero-D Growth Interface

## Cz growth of silicon in the [111] direction

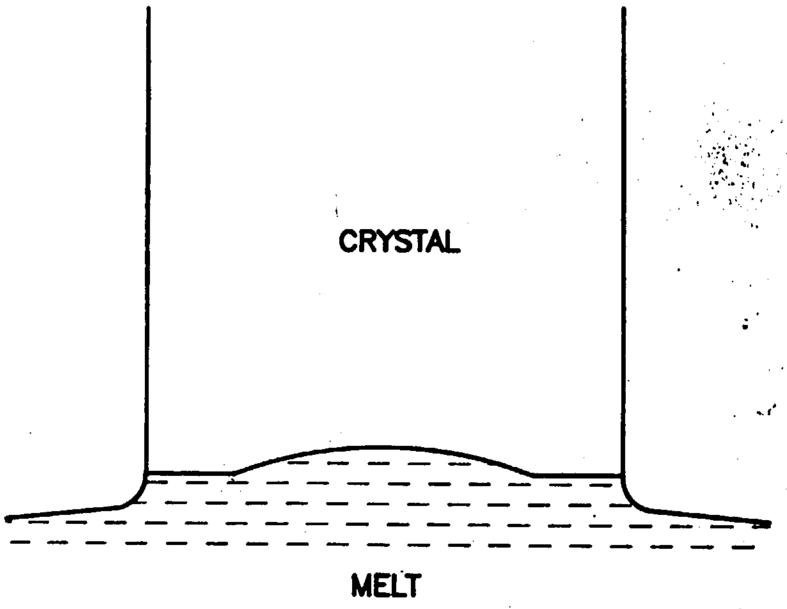

# Melt Convection

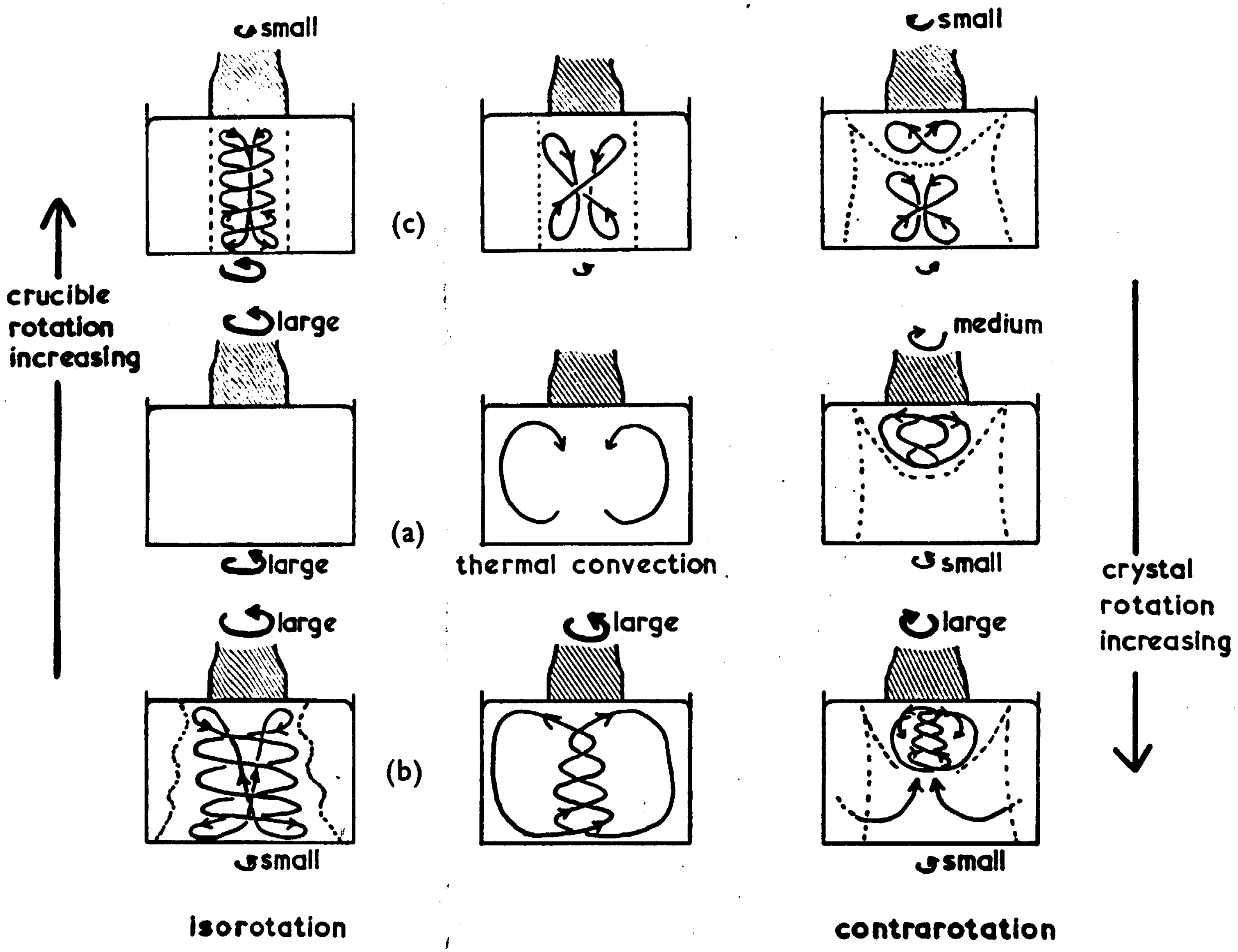

# Cz Silicon Ingot

## Silicon Casting, Inc.
## Diameters to 20 " $\phi$, zero-d

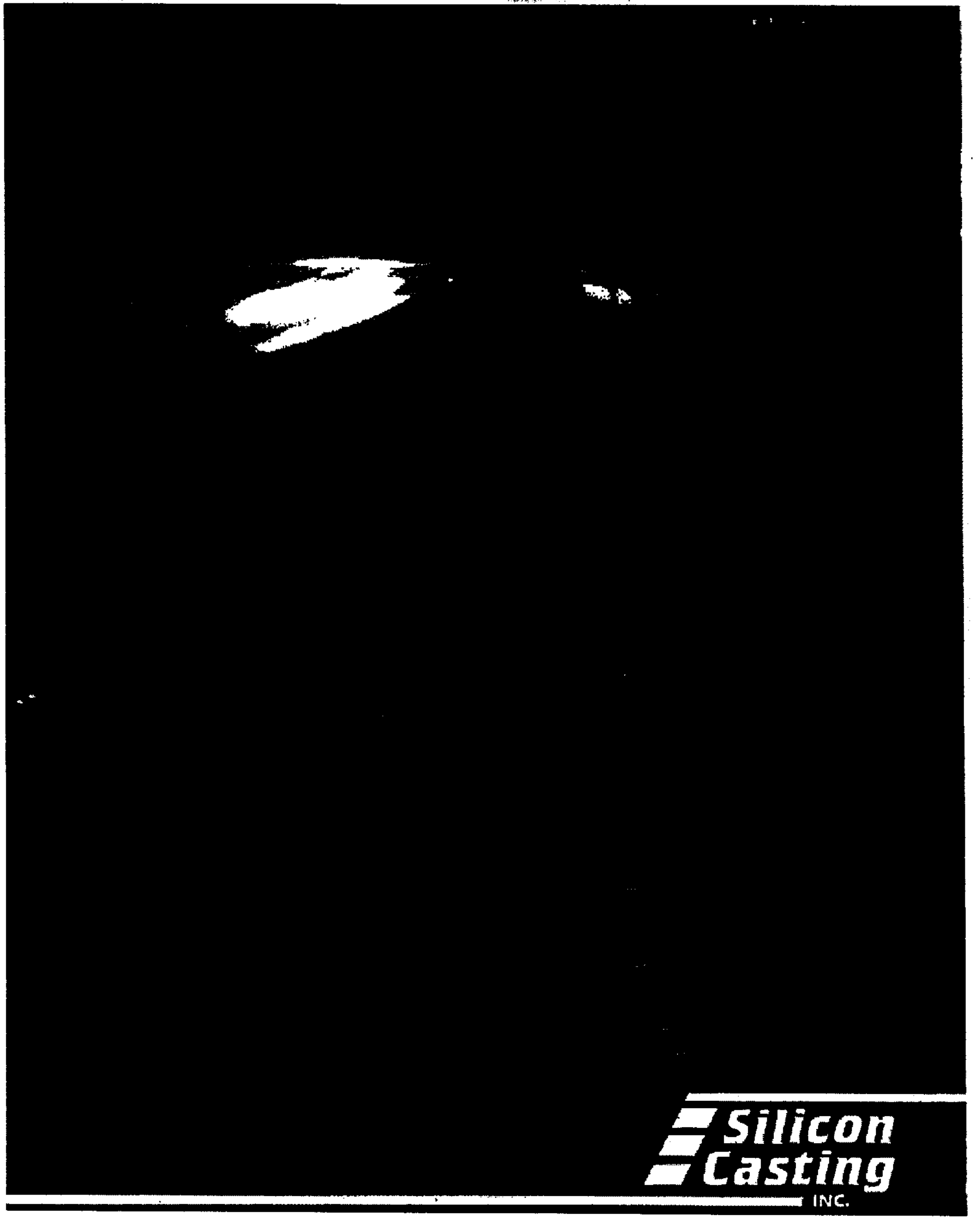

# Cz Silicon Grower

**Silicon Casting, Inc.**
**Diameters to 20 " $\phi$, zero-d**

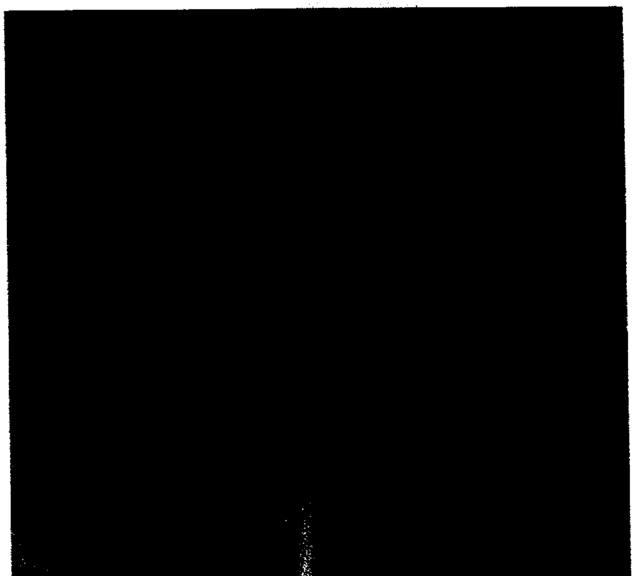

# Mockup of Silicon Crystal Pulling

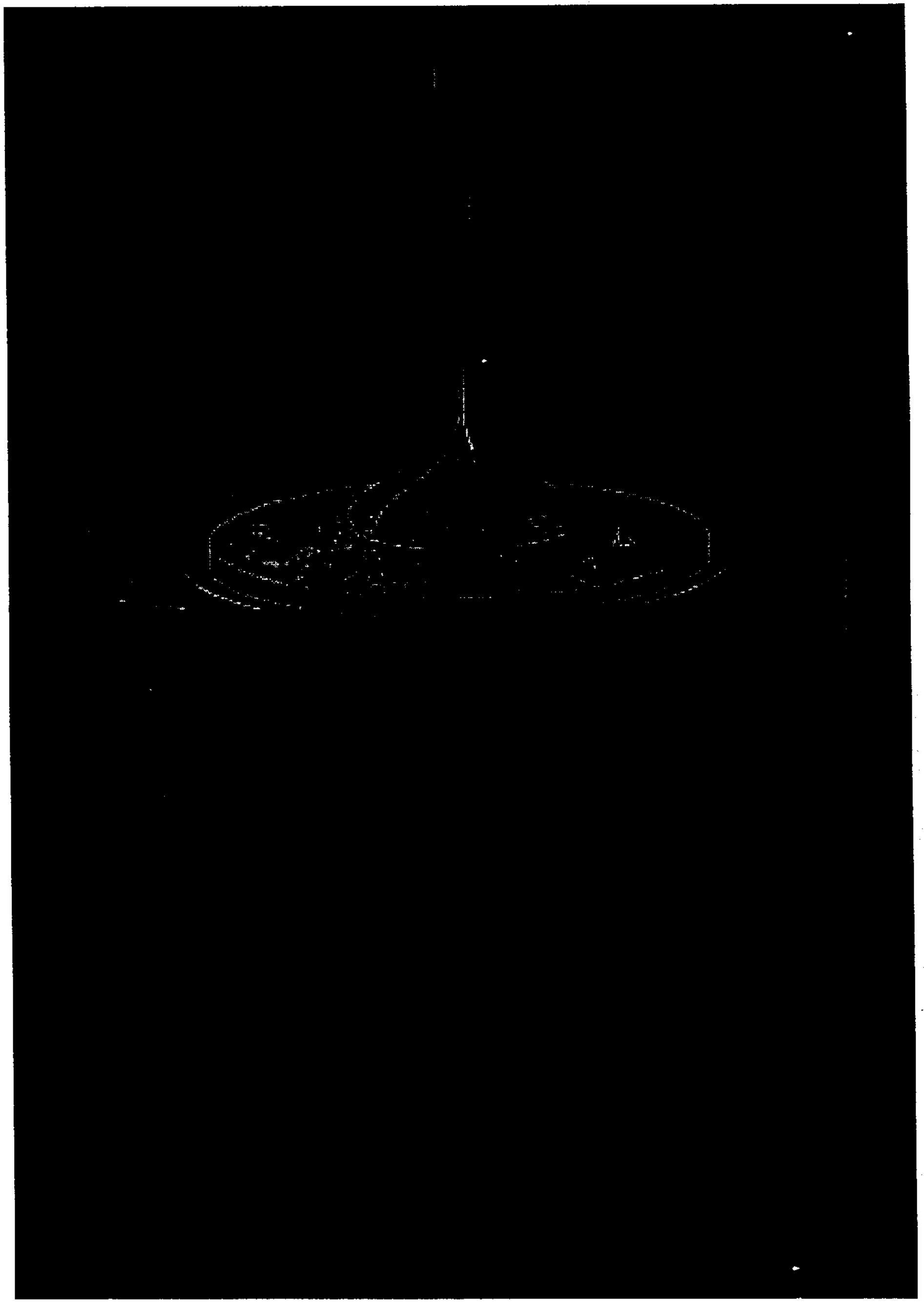

# Float Zone Silicon

## Unisil, diameters to 4 " ϕ

## Intrinsic - (as low as $10^{11}$ $cm^{-3}$)

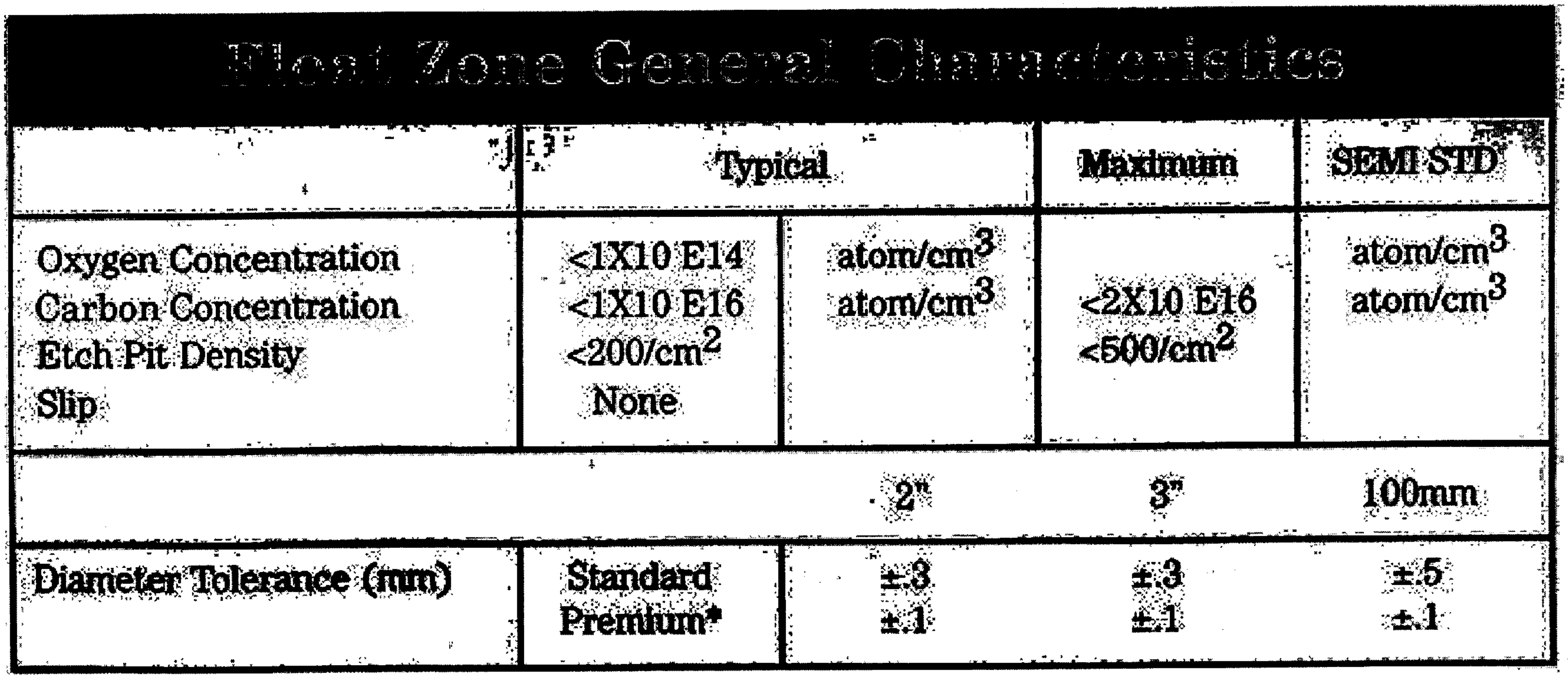

**Float Zone General Characteristics**

| | Typical | | Maximum | SEMI STD |
|---|---|---|---|---|
| Oxygen Concentration | <1X10 E14 | atom/cm$^3$ | | atom/cm$^3$ |
| Carbon Concentration | <1X10 E16 | atom/cm$^3$ | <2X10 E16 | atom/cm$^3$ |
| Etch Pit Density | <200/cm$^2$ | | <500/cm$^2$ | |
| Slip | None | | | |
| | | 2" | 3" | 100mm |
| Diameter Tolerance (mm) | Standard<br>Premium* | ±.3<br>±.1 | ±.3<br>±.1 | ±.5<br>±.1 |

# Float-Zone Silicon

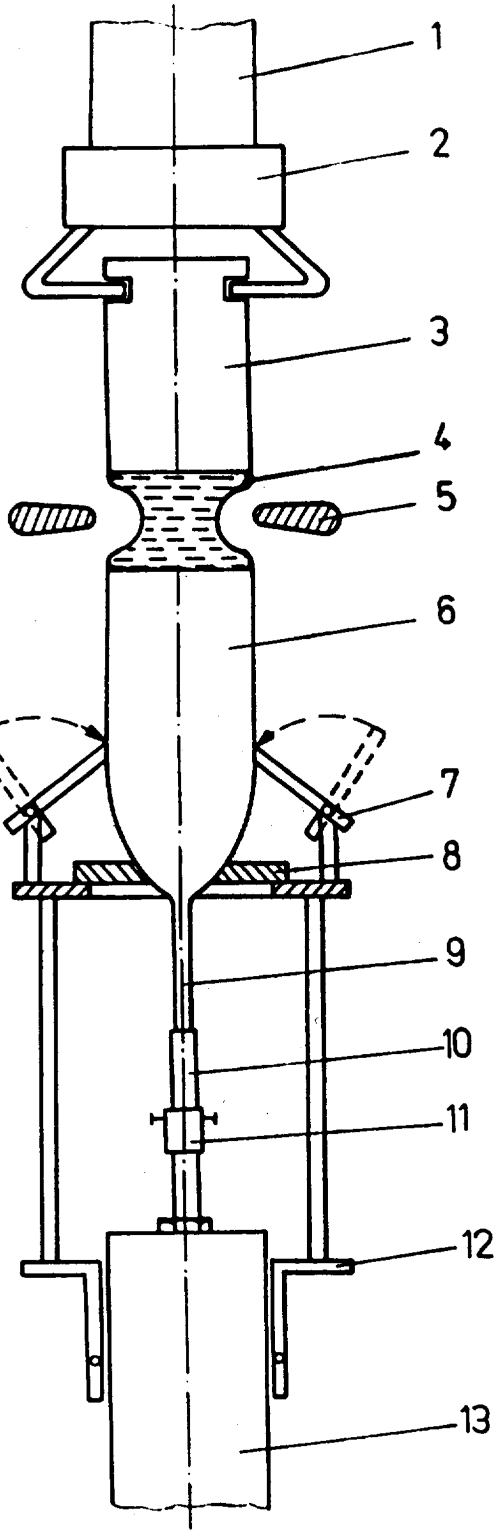

# Float Zone Silicon Molten Zone

Unisil, diameters to 4 " $\phi$

Intrinsic - (as low as $10^{11}$ cm$^{-3}$)

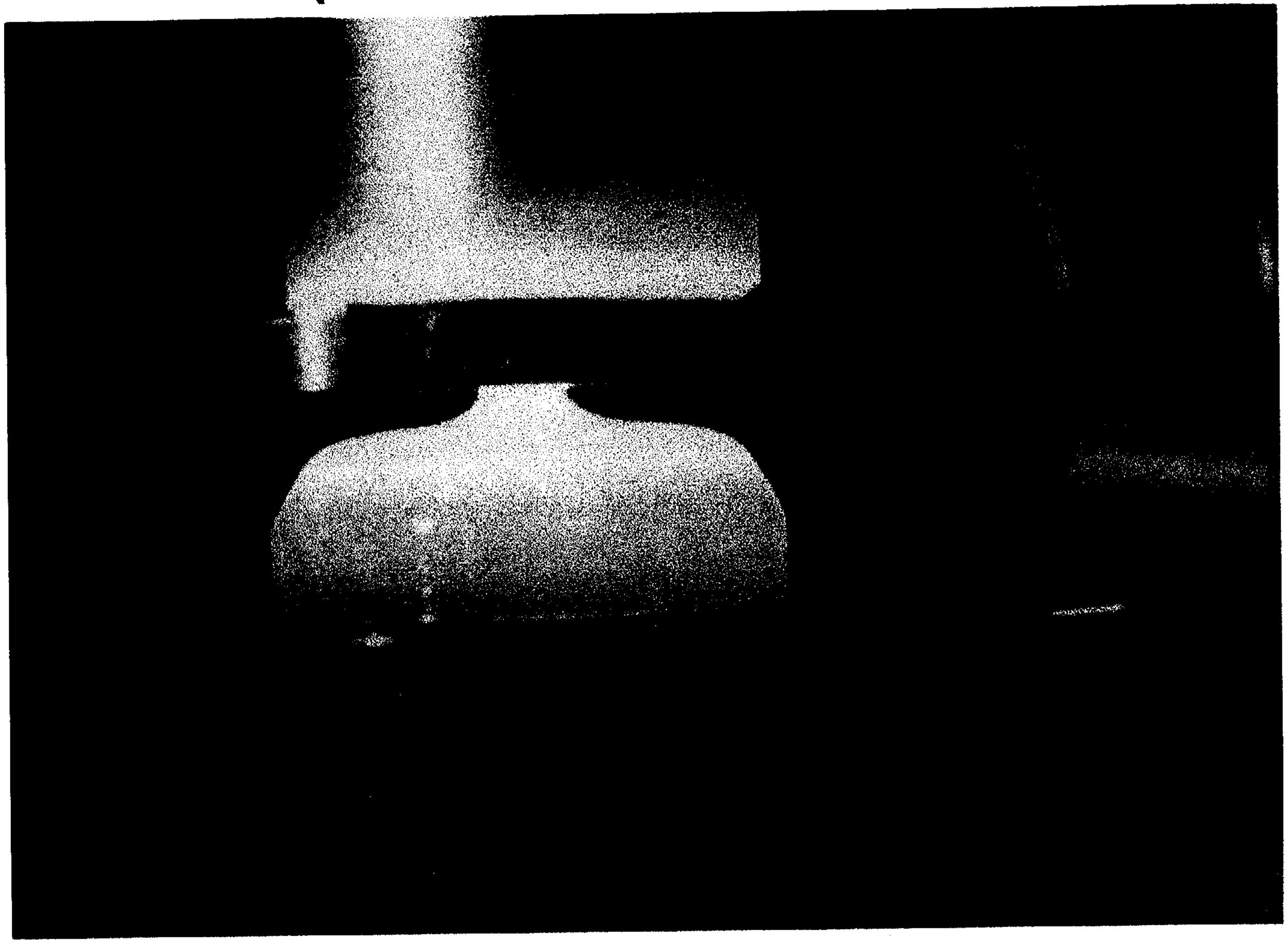

# Float Zone Silicon

**Unisil, diameters to 4 " $\phi$**

**Intrinsic - (as low as $10^{11}$ cm$^{-3}$)**

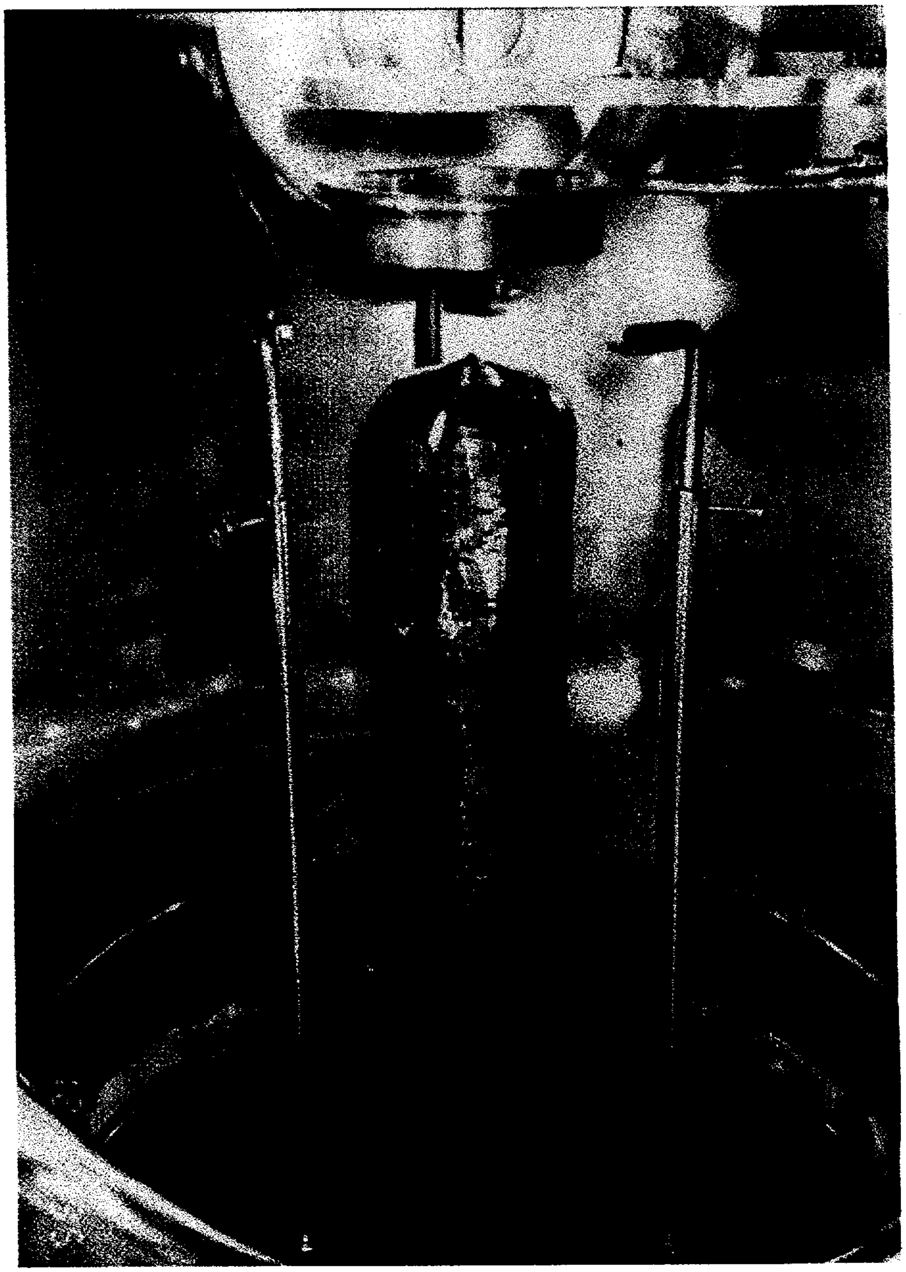

# Float-Zone Silicon Grower

# Phase Equlibria in MgO-Al$_2$O$_3$

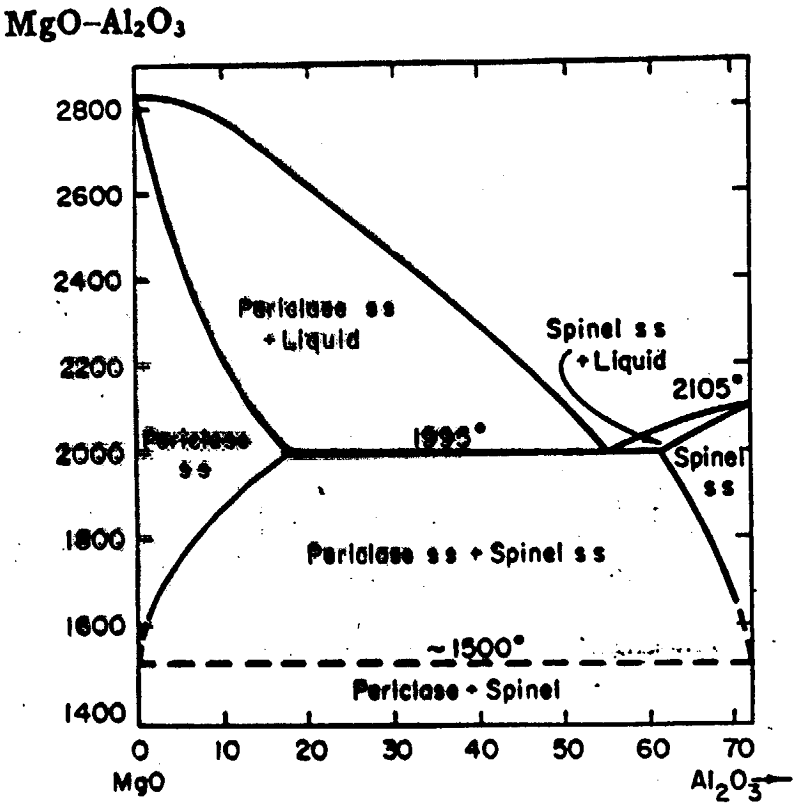

FIG. 259.—System MgO–MgO·Al$_2$O$_3$.

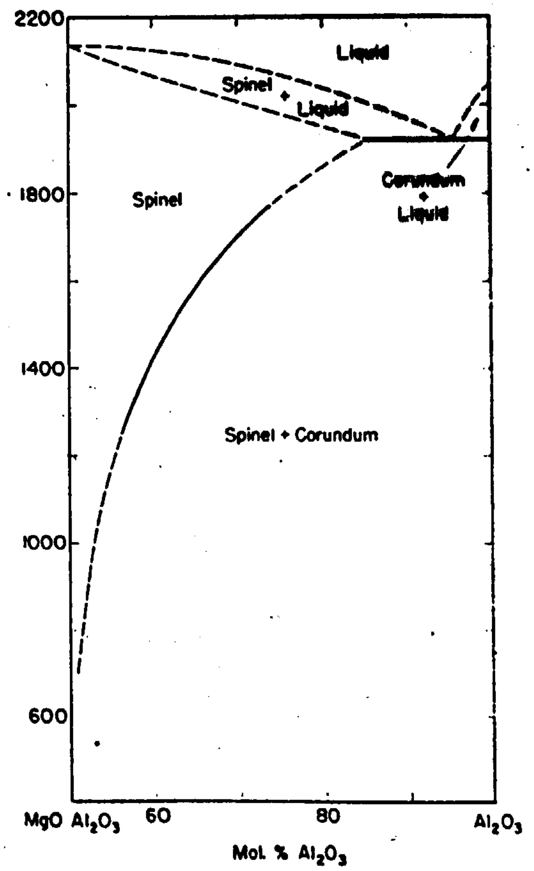

# HEM Growth of Spinel

- D. Viechnicki, F. Schmid and J. W. McCaulay 1972
- 5 cm ϕ x 5 cm high ingot, [100] seed

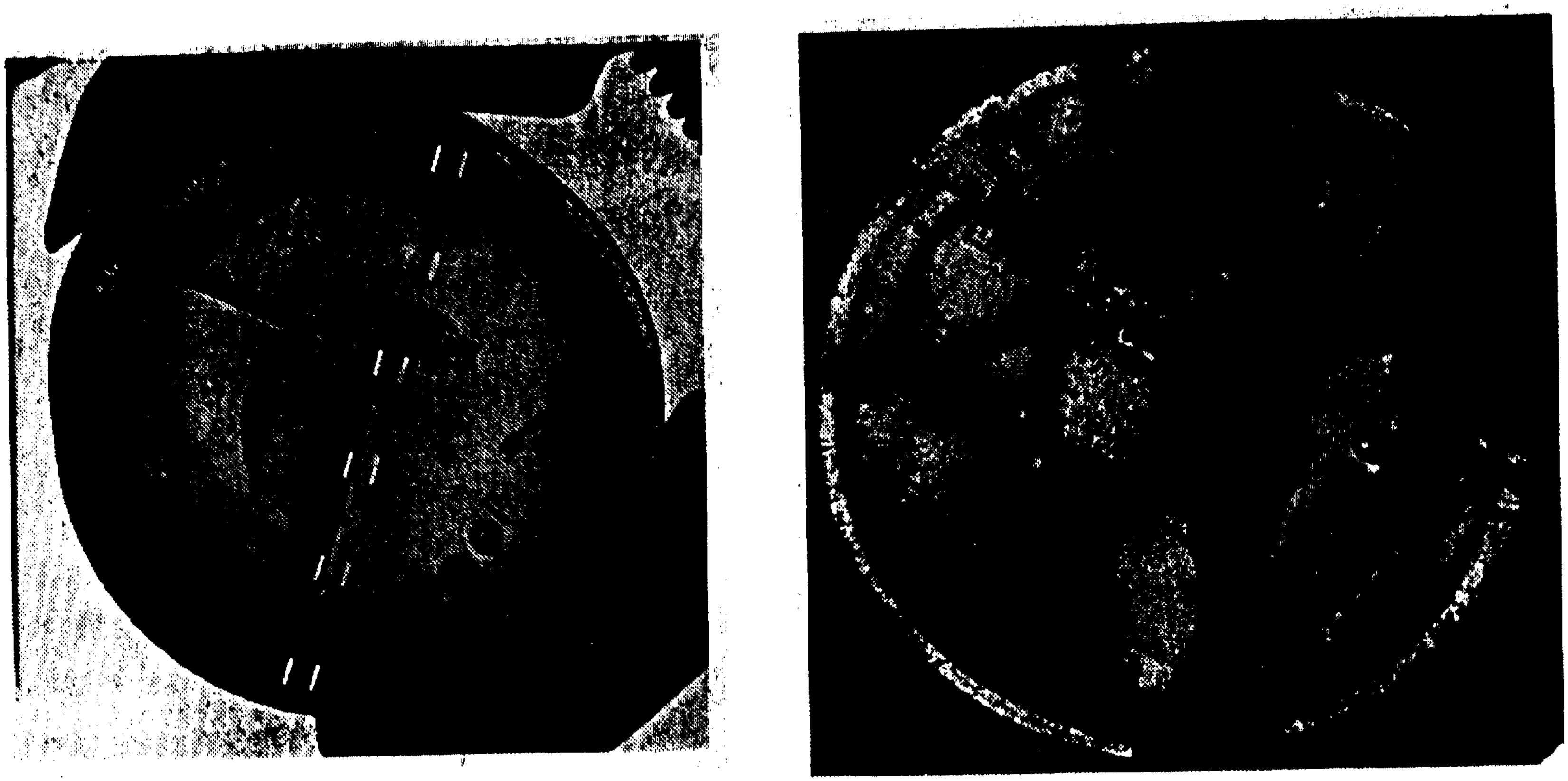

# Status of Spinel Crystal Growth

- Wide range of solid-solubility at high temps.
- Grown by HEM along [100] and [111]
- Molybdenum crucibles, 5 cm ϕ by 5 cm high
- MP = 2105°C using inert blanket
- Preferential loss of MgO (2 mole%) ► skin
- $Al_2O_3$ precipitates form around 1500°C during annealing due to continued MgO loss
- Cracking, compositional variations, and discoloration if charge is not fully oxidized